Volume 55
Number 5
3 February 2026
Pages 1925-2348

Dalton Transactions

An international journal of inorganic chemistry

rsc.li/dalton

ISSN 1477-9226

ROYAL SOCIETY OF CHEMISTRY

PERSPECTIVE

Satoru Tsushima and Koichiro Takao

Interactions of early actinides with biologically-relevant organic molecules including carboxylates, amino acids and proteins

Dalton Transactions

ROYAL SOCIETY OF CHEMISTRY

PERSPECTIVE

View Article Online
View Journal | View Issue

Cite this: *Dalton Trans.*, 2026, **55**, 1938

Interactions of early actinides with biologically-relevant organic molecules including carboxylates, amino acids and proteins

Satoru Tsushima *[a,b] and Koichiro Takao *[b]

This Perspective article reviews the current knowledge regarding the interaction of actinide elements with biomolecules, particularly amino acids, peptides, and proteins. We assess the significance of these interactions, especially in connection to nuclear waste disposal and the potential role of these interactions in the origin of life. Actinides have been observed to form stable complexes with carboxylate groups, resulting in oligomerization and affecting their environmental mobility. The text discusses the complex coordination chemistry of actinides, including the prevalence of hexanuclear An^{4+} clusters, and the implications of these findings for actinide transport and bioavailability as well as remaining challenges especially for mechanistic and thermodynamic aspects of this chemistry. Recent discoveries of lanthanide- and actinide-dependent enzymes, including methanol dehydrogenase and lanmodulin, suggest a potential for these elements to have been actively involved in early metabolic processes, rather than solely acting as environmental stressors. Despite the absence of direct evidence connecting natural reactors to the process of abiogenesis, a comprehensive understanding of actinide–biomolecule interactions is imperative for the evaluation of the nuclear geyser model and the resolution of the long-term challenges posed by the management of radioactive waste.

Received 8th October 2025,
Accepted 22nd December 2025

DOI: 10.1039/d5dt02408k

rsc.li/dalton

1. Background

Despite the persistent controversy surrounding abiogenesis, increasing evidence suggests life may have emerged in a radioactive environment, supporting the nuclear geyser model.[1,2] None of the previously-proposed hypotheses on the origin of life can provide the energy flux of ionizing radiation required to synthesize organic materials as demonstrated by the Miller–Urey-experiment.[3] By contrast, a natural nuclear reactor could have afforded high-energy flux which could have initiated chemical reactions to produce major biological molecules, including amino acids, nucleotides, and sugars from "raw" molecules (H_2O, N_2, and CO_2).[4] The nuclear geyser model asserts that natural nuclear fission reactor(s) on the Hadean Earth served as the driving force behind the emergence of life.

During this period, the isotopic proportion of fissile ^{235}U was as high as 20%, significantly higher than the current 0.72%. Under such circumstances, even low-grade uranium ore could have served as a functional nuclear reactor, given the presence of water as a neutron moderator. It should also be considered that the Moon was closer to the Earth in the Hadean Era, resulting in enormous tidal variations.

Natural nuclear reactors could have facilitated the circulation of material and energy, enabling chemical reactions leading to the synthesis of complex organic compounds including amino acids, peptides, and nucleobases. This process may have generated the earliest forms of metabolism, with uranium acting not just as fissile material but also as oligomeric catalyst and coordinating ion for prebiotic metalloenzymes.[5] Furthermore, increasing evidence for proteins and bacteria dependent on lanthanides or actinides[6–11] supports the notion that these elements played an essential role in early metabolism. Paleontological studies have unearthed the earliest eukaryotic fossil from the Paleoproterozoic Francevillian Group in Gabon, a region where natural nuclear reactor once existed.[12]

Taking into account these observations, and given the rich redox chemistry exhibited by actinides,[13] along with their remarkable coordinating ability,[14] their interaction with amino acids and subsequent oligomerization likely played a key role in prebiotic evolution and homochirality. Previous studies on the interaction between actinide and amino acid or with primitive peptide such as glutathione have not discussed the potential importance of these interactions in prebiotic systems.

Despite that the nuclear geyser model still remains hypothetical, and linking actinide with the origin of life being

[a]*Institute of Resource Ecology, Helmholtz-Zentrum Dresden-Rossendorf, Bautzner Landstraße 400, 01328 Dresden, Germany. E-mail: s.tsushima@hzdr.de*
[b]*Laboratory for Zero-carbon Energy, Institute of Integrated Research, Institute of Science Tokyo, 2-12-1 N1-32, O-okayama, Meguro-ku, 152-8550 Tokyo, Japan. E-mail: ktakao@zc.iir.isct.ac.jp*

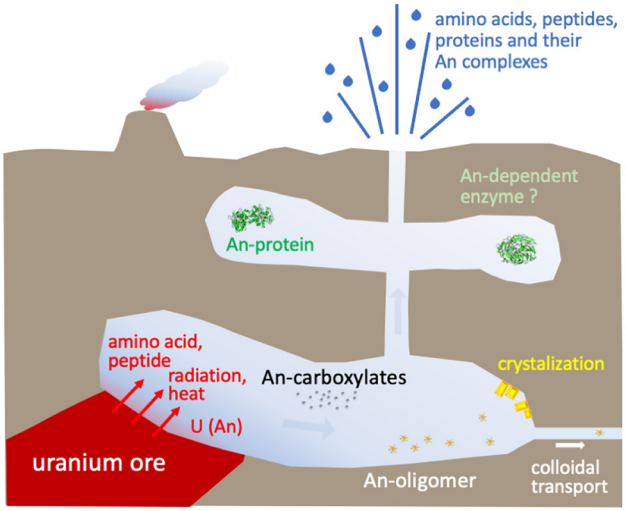

Fig. 1 Potential circulation routes of materials on Hadean to Eoarchean Earth as well as the roles of uranium, minor actinides, amino acids and their derivatives. This concept is based on a nuclear geyser model (see text and references therein), though the idea remains hypothetical. Scaling is enlarged arbitrarily for a selected group of objects.

controversial, it is also important to assess whether current biochemical knowledge of actinide-amino acid interaction aligns with the nuclear geyser model to test its validity. Fig. 1 depicts the circulation of materials on Hadean to Eoarchean Earth with the focus on uranium (+ minor actinides) and amino acids. This model proposes that natural nuclear reactors contributed to amino acid formation, which then facilitated the emergence of actinide carboxylates and related oligomers, transported in the geosphere. This process may have led to the formation of primitive proteins and enzymes potentially utilizing actinide ions.

This Perspective aims to provide a systematic review of past studies on the interactions of actinides with amino acids and proteins, to consider the broader implications of this rapidly developing field of research. Ultimately, we would like to help verify the nuclear geyser model from a chemical as well as biophysical perspectives rather than from an astronomical standpoint, and to suggest a research direction for that purpose.

2. Actinide coordination with carboxylates and amino acids

2.1. UO_2^{2+} interaction with amino acids

We initiate our discussions with the UO_2^{2+} ion, which is one of the most prevalent actinide ions. The complexation behaviour of UO_2^{2+} with general carboxylates ($RCOO^-$) has been thoroughly examined and documented,[15] and we do not go in depth to this direction in this Perspective. The interaction of UO_2^{2+} with amino acids (AAs) in aqueous solution has been the subject of extensive research.[16–19] Generally, ligand coordination to UO_2^{2+} is constrained to its equatorial plane, with a preferred coordination number of 5. The predominant interactions of UO_2^{2+} with AAs or proteins involve carboxylic groups, including those from the sidechains of Asp and Glu. Interactions with Tyr and His sidechains have also been reported.[18,20,21] Gas-phase experiments corroborate UO_2^{2+} coordination to the carboxylic group of Asp, the thiolate group of Cys, and the imidazole group of His.[22] It is also important to note that there are a number of examples of hydrogen bonding to the "yl"-oxygen of UO_2^{2+},[23] despite the "yl"-oxygen being generally inert. Such interaction frequently occurs in instances when UO_2^{2+} is situated within a hydrophobic environment, such as within a folded protein,[24,25] or when

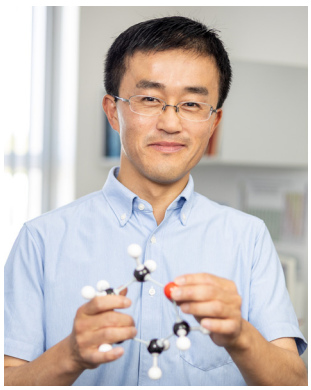

Satoru Tsushima

Prof. Satoru Tsushima completed his Ph.D. at the University of Tokyo in 1999. He assumed a faculty position at the Nagoya University in 2003, and later relocated to Stockholm University. In 2006, he was awarded a stipend from the Alexander von Humboldt foundation and moved to Grenoble, France, to work at the ESRF, and later became a senior scientist at Helmholtz-Zentrum Dresden-Rossendorf. Since 2017, he has also been a specially-appointed associate professor at the Institute of Science Tokyo. His current research interest pertains to the implementation of computational chemistry in the domain of actinide science (Photo copyright HZDR/C.Reichelt).

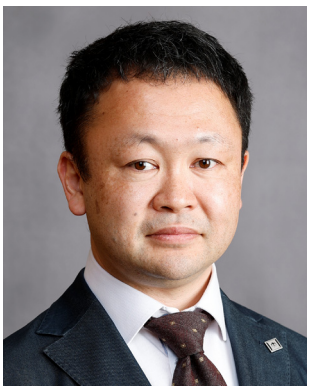

Koichiro Takao

Prof. Koichiro Takao (previously "Koichiro Mizuoka") finished his Ph.D in 2006 at Tokyo Institute of Technology ("Institute of Science Tokyo" today). He further explored actinide chemistry to develop a simple and versatile reprocessing principle at TokyoTech (2006–2008) and to deepen fundamental coordination chemistry of Th, U, and Np at HZDR (2008–2010). After accumulating his professional career as an assistant professor (2010–2015), he was appointed to an associate professor in the Laboratory for Zero-Carbon Energy, Institute of Science Tokyo in 2015. His research interest is still fundamental coordination chemistry of actinides, while it is closely related to nuclear fuel recycling, U harvesting from seawater, chemical utilization of depleted U, and flexible management of nuclear wastes.

hydrogen atoms from free AAs are in close proximity to UO_2^{2+}. In the case of the ternary complex of uranyl(VI)–Gly–fluoride, NMR spectroscopy has confirmed the presence of chelate-bonded Gly.[26]

Surprisingly, the number of reported crystal structures of UO_2^{2+} complexes with AAs is rather limited. A search of the Cambridge Structural Database revealed only two documented instances of crystal structures of UO_2^{2+} complexes with AA, both of which are Gly and its deprotonated form (Gly^-) through O^O bidentate coordination.[27,28] Other examples include its *N*,*N*,*N*-trimethylated derivative (*i.e.*, betaine),[29] and iminodiacetate.[30] An N^O bidentate coordination, which would be expected to form a stable 5-membered chelate ring according to conventional coordination chemistry, has not been observed in a crystal structure of UO_2^{2+}. However, this binding mode is plausible, as evidenced by the NMR spectrum of an aqueous UO_2^{2+}–Gly–F^- system,[26] and has been demonstrated with related ligands such as iminodiacetate,[31,32] nitrilotriacetate,[33] $EDTA^{4-}$,[33] and His-based Schiff bases.[34] Another O^O coordination mode of Gly and Ala is utilized to form infinite 1D coordination polymers of UO_2^{2+} (Fig. 2(A) and (B)), where *syn–syn* bridging of these AAs occurs between neighbouring UO_2^{2+} units,[23,35,36] thereby inhibiting further growth of the UO_2^{2+}–μ_3-O(H) 2D sheets of *meta*-schoepite, $(UO_2)_2O(OH)_6{\cdot}5H_2O$, (Fig. 2(C))[37] that initially form upon UO_2^{2+} hydrolysis.

2.2. An^{4+} carboxylates and hexamers (An = Th, U, Np, Pu)

While the formation of mononuclear complexes of actinide with simple AAs has little practical relevance and remains largely a subject of laboratory research, the oligomerization of actinides with AAs and other carboxylates is more pertinent to the nuclear industry and to the environmental concerns.

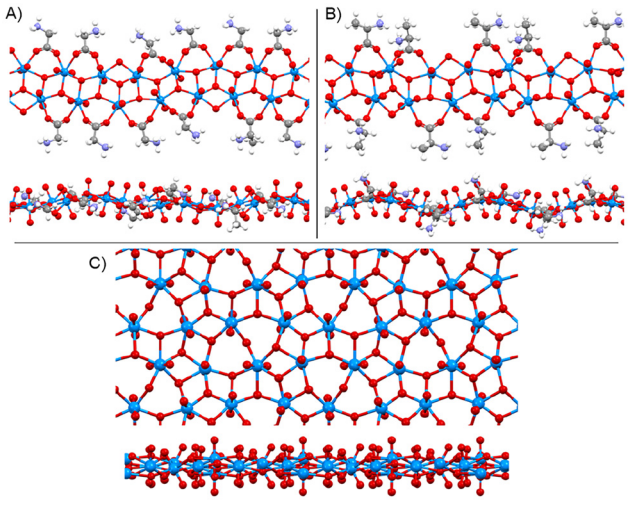

Fig. 2 Infinite 1D coordination polymers of UO_2^{2+} composed of uranyl pentagonal bipyramids that are chelated by Gly (A) and Ala (B) in a *syn–syn* bridging (top and side views) reported by Forbes and coauthors[35] and infinite 2D sheet of *meta*-schoepite, $(UO_2)_2O(OH)_6{\cdot}5H_2O$ (C), along *a*- and *b*-axes reported by Weller *et al.*[37]

While the hydrolysed UO_2^{2+} coordination polymers with Gly and Ala have been exemplified above, oligomerization and polymerization of actinides is more frequently observed in the tetravalent oxidation states (An^{4+}, An = Th, U, Np, Pu). This phenomenon can be attributed to the pronounced hydrolytic tendency of An^{4+}, which is characterized by the presence of high charge densities. These charge densities are conductive to promote polynucleation through olation and oxolation.[38] The final product resulting from the hydrolysis of An^{4+} is AnO_2(c), which exhibits fluorite-like crystal structure. This topic will be discussed in detail in the subsequent section.

In the presence of carboxylate ($RCOO^-$), it is necessary to consider the competition between the hydrolytic polynucleation of An^{4+} and coordination interactions of $RCOO^-$ with An^{4+}, that may occur in a concurrent manner. Although a variety of coordination manners of $RCOO^-$ are theoretically possible, the *syn–syn* bridging by μ-$RCOO^-$ is exclusively observed in the cases of An^{4+}. In the early era of actinide coordination chemistry, isolated compounds from An^{4+}–carboxylate systems were erroneously assigned to simple compound such as $[An(RCOO)_4]_n$, where the metal ions were supposed to be interconnected by μ-$RCOO^-$, to form infinite 1D coordination polymers.[15] Even in the aftermath of the hydrolysis of An^{4+}, the polymeric structure were considered to remain largely intact, with partial replacement of $RCOO^-$ by OH^-. Today, it is hard to accept such an infinite 1D coordination polymer to occur as a soluble species in mother liquors. In fact, already in 1920s, the presence of Th(IV) oligomeric species has been suggested through the study on the Th^{4+}–$HCOO^-$ system to propose the compound $[Th_3(OH)_5(HCOO)_6]{\cdot}A{\cdot}nH_2O$ (A = ClO_4, NO_3, HCOO, SCN, ClO_3) first by Weinland and Stark in 1926 [39] and later by Reihlen and Debus in 1929.[40]

Eight decades later, we have successfully identified the precise molecular and crystal structures of polynuclear complexes of Th^{4+} and U^{4+} with $HCOO^-$ by means of single crystal X-ray diffraction.[41] These An^{4+} compounds exhibit common molecular structures consisting of discrete hexanuclear complexes, $[An_6(\mu_3\text{-}O)_4(\mu_3\text{-}OH)_4(\mu\text{-}HCOO)_{12}(H_2O)_6]$ (An = Th, U; Fig. 3(A)), where μ_3-O^{2-}/OH^- are included as tripodal connectors for three An^{4+} ions to form an An^{4+} hexamer (Fig. 3(B)). The octahedral core of the $\{An^{4+}\}_6$ structure is further decorated by μ-$HCOO^-$, which serves to bind each pair of neighbouring An^{4+} ions. Note that the compositions of the compounds we identified are nearly double as those suggested in 1920s. This results in the following formula: $[Th_6(OH)_{10}(HCOO)_{12}]{\cdot}A{\cdot}nH_2O$ = $[Th_6(\mu_3\text{-}O)_4(\mu_3\text{-}OH)_4(HCOO)_{12}]{\cdot}2HA{\cdot}2(n{+}1)H_2O$, where some variations in co-crystallized salts/acids can be found. Furthermore, extended X-ray absorption spectroscopy (EXAFS) and UV-vis spectroscopy successfully confirmed the formation of these $[An_6(\mu_3\text{-}O)_4(\mu_3\text{-}OH)_4(\mu\text{-}HCOO)_{12}(H_2O)_6]$ complexes in aqueous solutions (Fig. 3(C) and (D)), thereby establishing a clear connection between solution chemistry and solid-state structures. Although the formation of such an An_6O_8 core unit has been previously observed in diphenylphosphate and triflate systems,[42,43] in which the

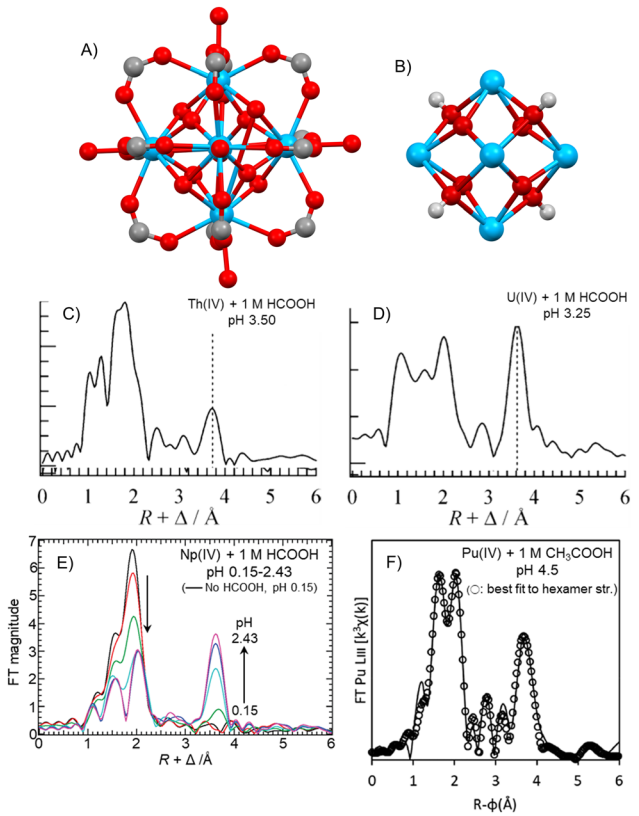

Fig. 3 Structural chemistry of An^{4+}–$RCOO^-$ hexanuclear complexes reported so far. Whole molecular structure of $[Th_6(\mu_3\text{-}O)_4(\mu_3\text{-}OH)_4(\mu\text{-}HCOO)_{12}(H_2O)_6]$ (A, where H atoms were omitted for clarity) and its An_6O_8 core (B) together with Fourier transforms of k^3-weighted L_{III}-edge EXAFS spectra of An^{4+} (An = Th (C, 50 mM),[41] U (D, 15 mM),[41] Np (E, 25 mM),[46] Pu (F, 3.9 mM)[51]) in aqueous solutions containing 1 M RCOOH (R = H, CH_3) under specific pH conditions. Panel (C), (D), (E), and (F) were reproduced from ref. 41, 46 and 51, respectively, with permission from Wiley-VCH GmbH (Copyright 2009) and American Chemical Society (Copyright 2012, 2022).

deprotonated phosphate diesters or triflate anions are located at the edges of the $\{An^{4+}\}_6$ octahedron in a manner analogous to μ-$HCOO^-$ of Fig. 3(A), research activities on polynuclear complexes of hydrolysed An^{4+} with μ-$RCOO^-$ and related organic molecules have been revitalized.

As a matter of fact, this class of chemistry was further expanded to the heavier tetravalent actinides, Np^{4+} and Pu^{4+}. In connection with our findings of the hydrolysed hexamers of Th^{4+} and U^{4+} decorated by μ-$HCOO^-$ described above,[41] and the following works with $PhCOO^-$ (ref. 44) and CH_3COO^-/$ClCH_2COO^-$,[45] we have explored solution coordination chemistry of Np^{4+} under the presence of $RCOO^-$ (R = H, CH_3) in aqueous systems by means of UV-vis and EXAFS.[46] Predominant formation of $[Np_6(\mu_3\text{-}O)_4(\mu_3\text{-}OH)_4(\mu\text{-}RCOO)_{12}]$ was commonly observed in both R = H, CH_3 systems of 1.00 M RCOOH at pH $\gtrsim$ 2 as pronounced by representative intermetallic interactions in Fourier transforms of the EXAFS spectra (Fig. 3(E)) at $R + \Delta$ = 3.80–3.81 Å and 5.39–5.40 Å for adjacent and diagonal pairs of Np atoms, respectively. The presence of the terminal H_2O observed in the X-ray structures with the lighter An^{4+} (Fig. 3(A)) could not be unambiguously confirmed in the case of Np^{4+} complexes due to uncertainty in the EXAFS analysis. The coordinating water molecules may not be present, considering the smaller ionic radius of Np^{4+} (0.98 Å, CN = 8) compared with Th^{4+} (1.05 Å for CN = 8, 1.09 Å for CN = 9) and U^{4+} (1.00 Å for CN = 8, 1.05 Å for CN = 9).[47] However, this issue remains controversial, as both the presence and the absence of an H_2O molecule in hexanuclear complexes of the smaller Pu^{4+} have been reported in the literatures (*vide infra*).[48,49] The EXAFS analysis of aqueous solutions revealed a distinction between the distances of Np–μ_3-O^{2-} (2.22–2.23 Å) and Np–μ_3-OH^- (2.42–2.43 Å). This observation is noteworthy, as such distinctions are often ambiguous in crystal structures due to the inherent disorder of μ_3-O^{2-}/OH^- as exemplified by $[Th_6(\mu_3\text{-}O)_4(\mu_3\text{-}OH)_4(RCOO)_{12}(H_2O)_6]$ (R = H, CH_3, CH_2Cl)[45] deposited under the absence of $NaClO_4$ in the mother liquors. An analogous Np^{4+} hexamer decorated by $PhCOO^-$ was also observed in an EtOH/aqueous 1 : 1 mixture, while this solid phase was characterized only by powder XRD.[50] Subsequent to the X-ray crystallographic studies on Pu^{4+} hexamers with Gly and 1,4,7,10-tetraazacyclododecane-1,4,7,10-tetraacetate (H_nDOTA^{n-4}), which we will discuss later,[48,49] the CEA group undertook an examination of solution coordination chemistry in an aqueous Pu^{4+}–CH_3COO^- system.[51] In a manner analogous to the Np^{4+} case,[46] the Pu_6O_8 cluster decorated by the *syn–syn* bridging CH_3COO^- such as $[Pu_6(\mu_3\text{-}O)_4(\mu_3\text{-}OH)_4(\mu\text{-}CH_3COO)_{12}(H_2O)_6]$ was found to be formed predominantly under the presence of 1 M CH_3COOH at pH 4.5 (Fig. 3(F)), where H_2O molecule capping each vertex of the $\{Pu^{4+}\}_6$ octahedral core was also included in the EXAFS fit with a fixed coordination number for each shell. In a manner analogous to Np^{4+}, $PhCOO^-$ also allowed to yield a Pu^{4+} hexanuclear cluster, $[Pu_6(\mu_3\text{-}O)_4(\mu_3\text{-}OH)_4(PhCOO)_{12}(H_2O)_4]$, wherein only eight $PhCOO^-$ are involved in the *syn–syn* bridging between neighbouring Pu^{4+} atoms, and the remaining four $PhCOO^-$ are either monodentate or bidentate-chelating to bind to a single Pu^{4+}.[50]

While the majority of reported works remain focused on Th^{4+} and U^{4+}, in contrast to the limited numbers of known examples of Np^{4+} and Pu^{4+}, several review articles are currently available that offer comprehensive summaries on the coordination chemistry of polynuclear An^{4+} complexes with $RCOO^-$ and polycarboxylates.[38,52–56] These two ligand systems, $RCOO^-$ and polycarboxylates, are closely related to each other, making it difficult to distinguish them distinctly. However, the former ($RCOO^-$) places greater emphasis on the fundamental aspects of this structural chemistry class, and it is also relevant to understanding the reaction mechanisms of AnO_2 colloid formation, especially for PuO_2 colloidal nanoparticles. The main concern of the latter (polycarboxylates) is the utilization of An_6O_8 core unit as building blocks of metal–organic frameworks (MOFs) mimicking non-radioactive tetravalent transition metal ions, most typically Zr^{4+}, to afford UiO-6*X* (*X* = 6, 7) type MOF structures.

In contrast to $RCOO^-$, the coordination chemistry of An^{4+} with AAs is even more limited despite their higher biological

relevance compared to $RCOO^-$. In the majority of instances, this coordination chemistry is exclusively confined to the systems with Gly. The $[An_6(\mu_3\text{-}O)_4(\mu_3\text{-}OH)_4(\mu\text{-}Gly^-)_x(\mu\text{-}Gly)_{12-x}(H_2O)_6]^{12-x}$ was obtained commonly for An = Th (x = 6)[57,58] and U (x = 0).[59] In these cases, the *syn–syn* bridging manner of the carboxylate moiety of Gly and/or its deprotonated form (Gly^-) followed that observed for $RCOO^-$ (Fig. 4 (A)). Using EXAFS, we observed predominant formation of $[Np_6(\mu_3\text{-}O)_4(\mu_3\text{-}OH)_4(\mu\text{-}AA)_{12}]^{y+}$ (AA = Gly, Ala, Cys; $0 \le y \le 12$) in aqueous solutions under acidic conditions even below pH 1 (Fig. 4(B)).[46] It is important to note that no significant effects of sidechains (R) of Ala (R = $-CH_3$) and Cys (R = $-CH_2SH$) have appeared in the actual Np^{4+} hexamer formation. The initial report on the Pu^{4+} version of the hexanuclear coordination clusters in this context is X-ray structure determination of $[Pu_6(\mu_3\text{-}O)_4(\mu_3\text{-}OH)_4(\mu\text{-}Gly)_{12}(H_2O)_6]^{12+}$ co-crystallized with Li^+, Cl^-, and crystalline water molecules,[48] where $\mu_3\text{-}O^{2-}/OH^-$ are not distinguishable due to their disorder. Each vertex of the $\{Pu^{4+}\}_6$ core is capped by a H_2O molecule ($Pu\text{–}O_w$ = 2.688 Å) to form a nine-coordination geometry around each Pu^{4+}. This is notable because the ionic radius of Pu^{4+} is smaller than that of Np^{4+}. Due to the zwitterionic nature of AAs in the charge-neutral state, the *syn–syn* bridging mode of their carboxylate group is offered in both the original ($H_3N^+\text{–}CHR\text{–}COO^-$) and the deprotonated ($H_2N\text{–}CHR\text{–}COO^-$) forms. This phenomenon underlies the formation of $[An_6(\mu_3\text{-}O)_4(\mu_3\text{-}OH)_4(\mu\text{-}AA^-)_x(\mu\text{-}AA)_{12-x}]^{12-x}$ (AA^-: deprotonated AA) even in acidic conditions, as evidenced in the Np^{4+} case.[46] However, the hydrolysis tendencies of An^{4+} of interest should also be taken into account.

The scarcity of knowledge regarding AA systems is not confined solely to An^{4+}; it also pertains to tetravalent Group 4 metal ions in the periodic table. This tendency is particularly evident in the case of Zr^{4+}, which has undergone extensive development in this direction, though the only known hexanuclear complexes with AA are those with Gly[60,61] and its *N*,*N*,*N*-trimethylated variant (*i.e.*, betaine).[62] In the former system, the assignment of the positions of H^+ on Gly remains ambiguous, as evidenced by the different formulas $[Zr_6(\mu_3\text{-}OH)_8(\mu\text{-}Gly)_4(\mu\text{-}Gly^-)_4(H_2O)_8]^{12+}$ and $[Zr_6(\mu_3\text{-}O)_4(\mu_3\text{-}OH)_4(\mu\text{-}Gly)_8(H_2O)_8]^{12+}$ in the articles from the same group. The reduced number of *syn–syn* bridging carboxylates compared with the An^{4+}–Gly systems described above would be ascribed to steric demand arising from the smaller ionic radius of Zr^{4+} (r_{Zr} = 0.84 Å, r_{An} = 0.96–1.05 Å at CN = 8).[47] In the latter case of

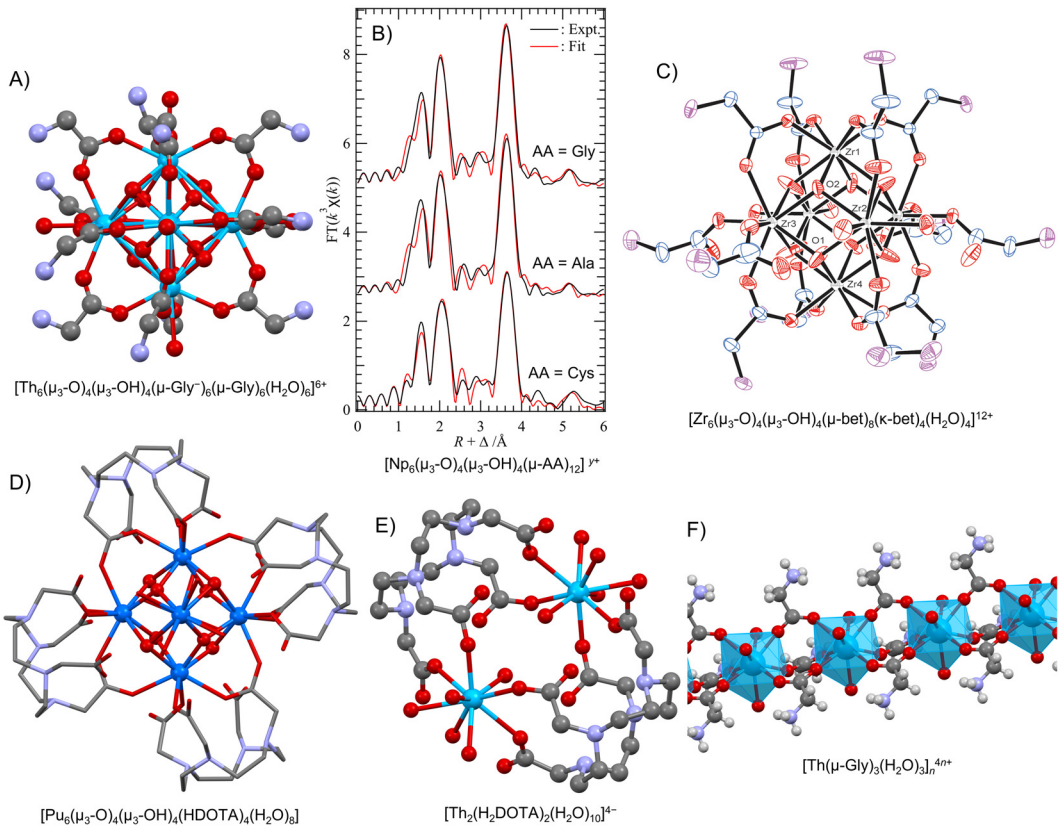

Fig. 4 Structural chemistry of M^{4+}–AA systems reported so far, where H atoms were omitted for clarity unless specified. (A) $[Th_6(\mu_3\text{-}O)_4(\mu_3\text{-}OH)_4(\mu\text{-}Gly^-)_6(\mu\text{-}Gly)_6(H_2O)_6]^{6+}$.[57] (B) Fourier transforms of k^3-weighted Np L_{III}-edge EXAFS spectra of $[Np_6(\mu_3\text{-}O)_4(\mu_3\text{-}OH)_4(\mu\text{-}AA)_{12}]^{y+}$ in aqueous solutions (AA = Gly, Ala, Cys; $0 \le y \le 12$).[46] (C) $[Zr_6(\mu_3\text{-}O)_4(\mu_3\text{-}OH)_4(\mu\text{-bet})_8(\kappa\text{-bet})_4(H_2O)_4]^{12+}$.[62] (D) $[Pu_6(\mu_3\text{-}O)_4(\mu_3\text{-}OH)_4(HDOTA)_4(H_2O)_6]$.[49,63] (E) $[Th_2(H_2DOTA)_2(H_2O)_{10}]^{4-}$.[63] (F) $[Th(\mu\text{-}Gly)_3(H_2O)_2]_n^{4n+}$.[57] H atoms in panels (A) and (C)–(E) and terminal CH_3 groups in panel (C) were omitted for clarity. Panel (B) and (C) were reproduced from ref. 46 and 62 with permission from American Chemical Society (Copyright 2012) and Elsevier (Copyright 2012), respectively.

betaine, the *N*-terminal of Gly was quaternarized by trimethylation to resolve the ambiguity problem of H^+, where the zwitterionic form of betaine, $(H_3C)_3N^+CH_2COO^-$, can be maintained during complexation. As a result, preparation and structural characterization of $[Zr_6(\mu_3\text{-}O)_4(\mu_3\text{-}OH)_4(\mu\text{-bet})_8(\kappa\text{-bet})_4(H_2O)_4]^{12+}$ (bet: betaine) in conjunction with its Hf^{4+} analogue proved to be successful, as demonstrated in Fig. 4(C). In this study, half of the water molecules present in the preceding Gly systems were substituted with monodentate betaine, κ-bet. We have also attempted to synthesize Zr^{4+} hexamers with other ordinary AAs such as Ala, Val, Cys, and Leu to simulate the An^{4+}–AAs coordination chemistry, but no crystalline deposits could be obtained.[62] The factors that disturb the crystallization of Zr^{4+} hexamers with these AAs could not be fully identified. Nevertheless, there is no rationale for prohibiting the formation of the M_6O_8 complexes with AAs other than Gly for any M^{4+}, including An^{4+}, in aqueous solutions. As previously mentioned, the predominant formation of Np^{4+} hexamers with Ala and Cys was already confirmed by EXAFS.[46]

In relation to AAs, 1,4,7,10-tetraazacyclododecane-1,4,7,10-tetraacetic acid (H_4DOTA) was employed to stabilize the hydrolyzed hexanuclear complexes of An^{4+}, $[An_6(\mu_3\text{-}O)_4(\mu_3\text{-}OH)_4(HDOTA)_4(H_2O)_8]$ (An = U, Np, Pu, Fig. 4(D)),[49,63] where its triply deprotonated form, $HDOTA^{3-}$, is involved in these An^{4+} hexamers. Only one out of three deprotonated carboxylates in each $HDOTA^{3-}$ is involved in the *syn–syn* bridging between the neighbouring An^{4+} ions, while the other two are bound to An^{4+} in a monodentate manner. Upon initial observation, it appears that the sole protonated carboxylic group in the $HDOTA^{3-}$ ligand is not committed to any chemical bond. However, a closer look into the structure reveals that it is hydrogen-bonded to μ_3-OH^-, coordinating H_2O, and crystalline H_2O. These interactions contribute ultimately to the stabilization of hexanuclear clusters which has reduced number of *syn–syn* bridging carboxylates compared with other $RCOO^-$ and AA systems described above. In contrast, neither intra- nor intermolecular interactions of any non-coordinating N atoms in the cyclen moiety of $HDOTA^{3-}$ occur in the crystal structures of $[An_6(\mu_3\text{-}O)_4(\mu_3\text{-}OH)_4(HDOTA)_4(H_2O)_8]$. Despite the potential of Th^{4+} to form a hexanuclear complex with carboxylates as exemplified above, an aqueous mixture of Th^{4+} and H_4DOTA resulted in the formation of a dimeric complex *via* H_2DOTA^{2-} crosslinkers between Th^{4+} ions, $[Th_2(H_2DOTA)_2(H_2O)_{10}]^{4-}$ = $[Th(H_2DOTA)(H_2O)_5]_2^{4-}$ (Fig. 4(E)), where no olation/oxolation of Th^{4+} were observed presumably due to its least hydrolytic nature among the An^{4+} series.[64] The similar trend can be observed in the weakest intensity of the Th···Th interaction at $R + \Delta$ = 3.70 Å in the EXAFS spectrum of the Th^{4+}–$HCOO^-$ system (Fig. 3(C)) compared with those of other An^{4+} (Fig. 3(D)–(F)), indicating the least stability of $[Th_6(\mu_3\text{-}O)_4(\mu_3\text{-}OH)_4(\mu\text{-}RCOO)_{12}(H_2O)_6]$ among the An^{4+} series. A ClO_4^- salt of $[Th(\mu\text{-}Gly)_3(H_2O)_3]_n^{4n+}$ coordination polymer of Fig. 4(F) without hydrolysis of Th^{4+} was also yielded in a relatively acidic system at pH 1.0 as an initial condition, although it is generally difficult to identify the final pH of the mother liquor after slow evaporation of the solvent for crystal deposition.[57]

To date, the previous studies on actinide hexamers have exclusively focused on structural chemistry, because molecular structures of such polynuclear species are the most distinctive feature of this class of coordination compounds. EXAFS is a valuable tool for the analysis of the structures of chemical species that are present in solution. However, through this method, only the averaged radial distributions of coordinating and related atoms around a central metal may be obtained, whereas it is hard to get any information about angular functions of atomic coordinates of interest, unless specific multiple scattering is available in a system of interest. SCXRD, in contrast, is the most powerful technique for precise structure determination, and therefore, is widely employed. However, as illustrated by our preliminary trials for Zr^{4+}–AA systems,[62] crystallization of a coordination compound of interest often appears to be rather challenging. Furthermore, even if crystallization is successful, the subsequent structural analysis of such an intricated compound is not always straightforward. Mainly due to crystallinity issues and remarkable disorder in atomic coordinates, the structure refinement often needs to be compromised by treating some or all non-H atoms solely with isotropic temperature factors and/or by excluding H atoms assignments. It is noteworthy that, despite the fact that a typical hexanuclear structure of $[An_6(\mu_3\text{-}O)_4(\mu_3\text{-}OH)_4(\mu\text{-}RCOO)_{12}]$ is basically charge-neutral, there has been no reported crystal structure composed solely of actinide hexamer units. Instead, the reported structures invariably involve salts/acids (cations: $N_2H_5^+$, Na^+, Li^+, H^+; anions: ClO_4^-, NO_3^-, Cl^-, $HCOO^-$, SCN^-, ClO_3^-, *etc.*) and/or solvent molecules. While these additional species do not directly interact with An^{4+}, they are nevertheless likely to play important roles to hold the $[An_6(\mu_3\text{-}O)_4(\mu_3\text{-}OH)_4(\mu\text{-}RCOO)_{12}]$ molecule through non-covalent interactions, most typically hydrogen bonding, to construct its whole crystal structure for successful deposition of a compound of interest. Accordingly, the selection or design of a co-crystallizing salt, acid, and/or solvent should be made with the objective of facilitating the crystallization of An^{4+} polynuclear species and to further exploring the structural chemistry of hydrolytically-polymerized discrete An^{4+} coordination clusters decorated by carboxylate-based ligands.

In this context, the observed difficulty in crystallization in the AA systems can be attributed to the variable total electric charge of the M_6O_8 clusters, arising from degree of freedom of protonation/deprotonation at the terminal amino groups. Our quaternarization approach for the terminal N atom of AAs to immobilize the positive charge on it would be straightforward to resolve this issue even in An^{4+}–AA systems.[62] Indeed, *N*,*N*,*N*-trimethylated AA derivatives have already been prepared as bis(trifluoromethylsulfonyl)imide (Tf_2N^-) salts,[65] while the original aim of that work was development of a new class of AA-based ionic liquids. Although deprotonation from such AA-derivatives to liberate them from Tf_2N^- counter anion is still required for utilization of such zwitterionic betaine-type AAs, exploration of the structural chemistry of An^{4+} hexamers with AAs could be anticipated in such a manner.

To the best of our knowledge, the sidechains of Ala (R = $-CH_3$) and Cys (R = $-CH_2SH$) play only a bystander role during

the formation of Np^{4+} hexamers in aqueous solutions (Fig. 4 (B)).[46] Due to the limited exploration of An^{4+}–AA systems, the impact of the sidechains of AA on the coordination chemistry of An^{4+} remains to be elucidated. This is particularly evident for acidic AAs, such as Glu (R = $-C_2H_4COOH$) and Asp (R = $-CH_2COOH$), that comprise carboxylates within their sidechains. In the case of peptides and proteins, in which the carboxylic groups of AAs on the backbone are no longer available for coordination after their condensation with the $-NH_2$ of the neighbouring AA to form peptide bonds, the presence of carboxylic groups on the sidechains increases its significance. As a matter of fact, the EXAFS study by Daronnat *et al.* reported that Pu^{4+} forms a Pu_6O_8 cluster after binding to a wild-type calmodulin peptide, CaMWT (DKDGDGYITTKE).[66] This finding was confirmed by Pu···Pu interactions at $R + \Delta$ = 3.8 Å and 5.2–5.3 Å, which are representative signatures of the An^{4+} hexamers (see Fig. 3(C–F) and 4(B)). Subsequent molecular dynamics simulations suggested that Pu^{4+} can be solvated by H_2O molecule(s) even after being captured by the coordination site of CaMWT. This process enables the initiation of the hydrolysis of Pu^{4+} to form the Pu_6O_8 structure. In contrast, this phenomenon was not observed when another calmodulin peptide with a mutation, CaME (DKDGDGYIEAAE), was employed. In this case, no H_2O was found to enter the coordination sphere of Pu^{4+}. Despite the lack of comprehensive picture depicting the final accommodation of the Pu_6O_8 core within CaMWT, this work clearly represents importance of sidechains of AAs in the An^{4+} coordination chemistry. Herein, interconnections between the fundamental coordination chemistry of small molecular structures of An^{4+} with organic substances and extended biologically-relevant systems such as peptides and proteins have been established.

An An^{4+} hexanuclear complex commonly contain an An_6O_8 core unit, where all An^{4+}–O^{2-}, An^{4+}–OH^-, and An···An distances follow those in the $Fm\bar{3}m$ fluorite-like AnO_2 crystalline phases (U–O: 2.368 Å, U···U: 3.866 Å in UO_2; Th–O: 2.424 Å, Th···Th: 3.958 Å in ThO_2).[38] Therefore, a minimal AnO_2 crystalline unit can be postulated to be isolated within a hexanuclear complex, wherein all twelve edges of the AnO_2 unit cell are occupied by $RCOO^-$ to inhibit further hydrolytic interactions of incoming An^{4+} to μ_3-O^{2-}/$-OH^-$. The decoration of the surface of the An_6O_8 core with $RCOO^-$ efficiently terminates the crystal growth into bulk AnO_2, and eventually prohibits its deposition. Indeed, the presence of $RCOO^-$ enables the preparation of aqueous solution samples with An^{4+} concentrations as high as $\geq 10^{-2}$ M, as exemplified in Fig. 3 and 4. This concentration level is significantly higher than that of the original aqueous solubility of An^{4+} (*e.g.*, $\lesssim 10^{-8}$ M at pH > 4 for An = Pu), which is expected from their hydrolytic nature.[67] This finding has critical implications for the concept and strategy for geological disposal of nuclear waste. In relation to this subject, the CEA group has investigated the growth of the PuO_2 colloidal nanoparticles from the perspective of H/D kinetic isotope effects (KIE). Formation of the Pu_6O_8 cluster occurs during the early stage of the reaction, followed by an O–H bond cleavage (probably at μ_3-OH^- of the hexamer) as a rate-determining step.[68]

Now, a fundamental question emerges from these observations; does An^{4+} undergo further hydrolytic oligomerization from the An_6O_8 unit to ultimately form AnO_2 nanoparticles? If so, how? This mechanistic matter is critically responsible for the solubilization of An^{4+}, which is generally believed to be immobilized as sparingly soluble AnO_2 phase. Furthermore, it is important in evaluating actinide transport in the geosphere following the disposal of nuclear waste in deep underground repositories. While there have been DFT calculations that have simulated tri-, tetra-, hexa-, and 16-nuclear hydrolyzed Pu^{4+} clusters decorated by CH_3COO^-, a plausible oligomerization process is yet to be concluded through experiments.[51] Fig. 5 summarizes An^{4+} oligomer structures that have been characterized to date. The $Pu_{16}O_{23}$,[69] $Pu_{22}O_{32}$,[69] and $Pu_{38}O_{56}$ [69–71] clusters deposited from aqueous mother liquors were identified by X-ray crystallography, where Cl^- was employed instead of carboxylates to afford higher nuclearities of Pu^{4+} in these oligomers. However, no clear evidence of oligomeric nanostructures other than the Pu_6O_8 clusters in the reaction process was obtained at this time, implying either the absence or minor contribution of the larger oligomers during the formation of the PuO_2 nanoparticles.[72] In the case of U^{4+}, Falaise *et al.* obtained a hydrolysed 38mer after solvothermal treatment under controlled hydrolytic conditions in THF.[73] This $U_{38}O_{56}$ cluster bears a striking resemblance to the chloro-decorated Pu^{4+} 38mer described above, while a mixed ligand system comprising $PhCOO^-$ and Cl^- has been strategically employed to regulate the growth of UO_2. Additionally, Mazzanti's group detected more diverse U^{4+} oligomers with 6, 13, 16, 24, and 38-nuclearities in the $PhCOO^-$–Cl^- mixed ligand systems under the presence of a limited amount of H_2O in non-aqueous solvents such as CH_3CN and pyridine.[74] The 10, 12, and 22mers of U^{4+} were also suggested to occur in the reaction mixture. In general, the detection of some oligomers with specific numbers of metals should be regarded as merely a "snapshot" and their presence should not be overinterpreted. On the other hand, Pu^{4+} has been observed to exhibit a greater tendency for colloidal formation and migration,[75] as evidenced by the 1.3 km Pu transport observed at the Nevada nuclear test site.[76] Therefore, it is highly probable that U^{4+} and Pu^{4+} undergo distinct polymerization processes. It is worthwhile that, in most cases, the An_6O_8 core unit of the smallest unit of the fluorite-like crystalline AnO_2 are included in the reported An^{4+} hydrolysed oligomers with the higher nuclearities as highlighted in Fig. 5. A comprehensive understanding of the tendency of olation and oxolation of An^{4+} remains elusive, particularly in the context of variation among different actinides.[77] Further investigation in this area is necessary to gain a more comprehensive understanding of these phenomena.

Besides the mechanistic features described above, it is also mandatory to compile chemical thermodynamic data of An^{4+} hydrolysed oligomers, particularly those of hexamers, to quantitatively and universally comprehend the phenomena occurring within the aqueous system of interest. This encompasses the behaviour of An^{4+} in relation to additional concerns, such as adsorption and migration behaviour of An^{4+} in natural

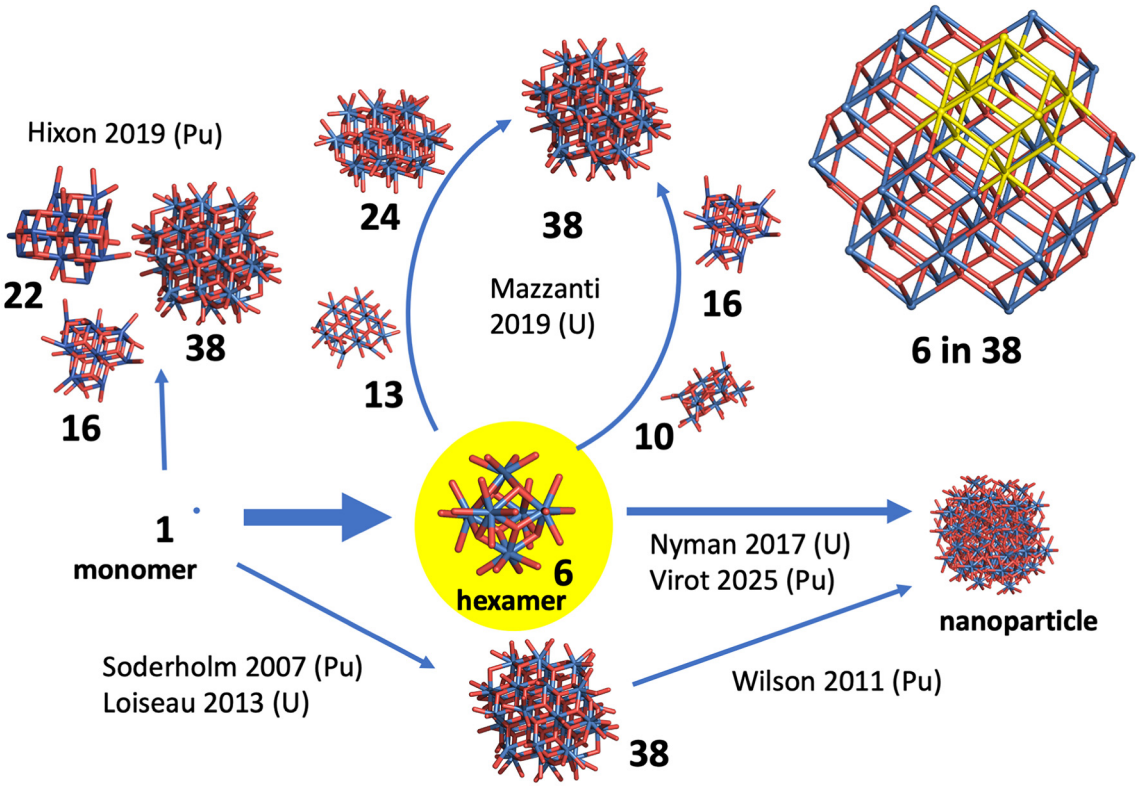

Fig. 5 Previously identified An^{4+} (An = U and/or Pu) oxo/hydro oligomers relevant to further polymerization and nanoparticle formation. Numbers in bold indicate the number of actinides within each oligomer. Only species relevant to aqueous chemistry are depicted. The inset at the top right shows the structure of $\{An\}_{38}$ core, with a single hexamer unit highlighted in yellow. The figure is based on the works by Nyman,[59] Hixon,[69] Soderholm,[70] Loiseau,[73] Wilson,[71] Virot,[72] and Mazzanti.[74]

environments related to the nuclear waste disposal. The stability constants of the An^{4+} oligomers exemplified above represent the most fundamental data necessary to predict the predominance of each species under specific conditions. In particular, the formation of an *n*-nuclear An^{4+} cluster is promoted in proportion to the *n*-th power of its concentration, more correctly "activity", in accordance with the mass action law. Therefore, simulating the solution chemistry of An^{4+} at micro- or nano-molar levels under the presence of carboxylate-based ligands is of crucial interest. However, to the best of our knowledge, virtually no research work has been done in this area, in contrast to extensive body of work on structural chemistry. We have previously established the stability constants of $[Np_6(\mu_3\text{-}O)_4(\mu_3\text{-}OH)_4(\mu\text{-}RCOO)_{12}]$ (R = H, CH_3) in conjunction with the related monomeric species, $[Np(RCOO)(OH)_2]^+$, which functions as a precursor for the Np^{4+} hexamer as outlined below:

$$6\ Np^{4+} + 12\ RCOO^- \rightleftarrows [Np_6(\mu_3\text{-}O)_4(\mu_3\text{-}OH)_4(\mu\text{-}RCOO)_{12}] + 12\ H^+ \quad (1)$$

$$Np^{4+} + RCOO^- \rightleftarrows [Np(RCOO)(OH)_2]^+ + 2\ H^+ \quad (2)$$

R = H, $\log \beta_{6,12,-12} = 42.7 \pm 1.2$ and $\log \beta_{1,1,-2} = 2.51 \pm 0.05$; R = CH_3, $\log \beta_{6,12,-12} = 52.0 \pm 0.7$ and $\log \beta_{1,1,-2} = 3.86 \pm 0.03$, where $\log \beta_{n,l,m}$ is the logarithmic gross stability constant of a Np^{4+}–$RCOO^-$–H^+ ternary complex with stoichiometries of these components denoted by *n*, *l*, and *m*, respectively. Based on these thermodynamic data, the speciation diagram for each system was successfully plotted as illustrated in Fig. 6(A) and (B),[46] where predominant formation of the Np^{4+} hexamers is predicted to start even under acidic conditions below pH ~ 2. In Fig. 6(C), pH dependencies of Np^{4+} solubility under the presence of $HCOO^-$ or CH_3COO^- under different concentration levels (10 mM, 1 M) were calculated from the above stability constants plus hydrolysis data of Np^{4+} available in the literature,[64] and overlaid on that of Np^{4+} hydrous oxide comprehended by Neck and Kim.[67] Note that the aqueous solubility of Np^{4+} is significantly enhanced especially in the acidic region after loading $RCOO^-$, while these conditions have been arbitrarily selected for simulation. No thermodynamic data are available for any An^{4+}–AA systems even today despite its higher biological relevance and stronger complexation tendency with metal ions including An^{4+}. Further research in the field of thermodynamics is necessary to ascertain the significance of actinide oligomers in environmental contexts.

3. Actinide and peptide

The concept of employing peptides to facilitate the recovery of metals, or at the very least to synthesize metal–peptide com-

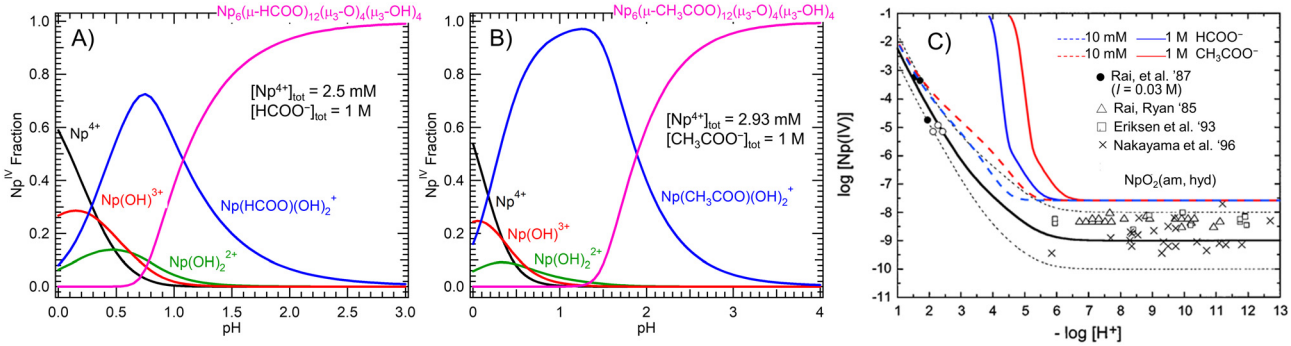

Fig. 6 Speciation diagrams of Np^{4+}–$RCOO^-$ systems (R = H (A), CH_3 (B))[46] as a function of pH together with logarithmic solubility of Np^{4+} in aqueous solutions (C) under absence (black)[67] and presence of $RCOO^-$ (R = H (blue), CH_3 (red); $[RCOO^-]$ = 10 mM (dashed), 1 M (solid))[46] at different pH. Panel (A) and (B) were reproduced from ref. 46 with permission from American Chemical Society (Copyright 2020). Panel (C) was adapted from ref. 67 with permission from De Gruyter Brill (Copyright 2001).

plexes, traces back to the early 1960s.[78] The majority of proteins involved in essential biochemical processes depend on metal cofactors to execute their functions. Therefore, preliminary research on metal-binding proteins frequently relied on metalloprotein and metalloenzyme studies to gain insights from nature's wisdom. In this context, the interactions between lanthanides/actinides and peptides have received much less attention, primarily due to the absence of any metalloprotein that utilize lanthanide/actinide, until Ln-dependent metalloenzyme was first discovered in 2011.[6]

Glutathione (GSH) is one of the simplest peptides consisting of just three amino acids (Glu, Cys, Gly) and known to be ubiquitous and found in all cells of the body. Kretzschmar *et al.*[79] conducted a study on the interaction between GSH and uranium(VI). The primary inquiry concerns the manner in which U(VI) binds with GSH. It has been determined that this binding occurs through the involvement of a carboxylic group, rather than a thiol group. This finding is consistent with the earlier study by Fahmy *et al.*,[80] who employed isothermal titration calorimetry (ITC) to investigate the interaction between the two substances. Furthermore, Kretzschmar *et al.* observed the reduction of U(VI) to U(IV) in the presence of GSH *via* an intermolecular mechanism in an aqueous medium *in vitro*. This process induced the formation of nanocrystalline, mixed-valence uranium oxide particles. Kretzschmar *et al.* also studied the interaction between U(VI) and glutathione disulfide (the disulfide complex of two glutathione molecules, GSSG) to observe the formation of the insoluble, low-mobility U(VI)–GSSG complex.[81] Fahmy *et al.*[80] studied the detoxification of uranium by GSH, using anaerobically grown *Lactococcus lactis* as a model organism. Their data suggest that the primary detoxification mechanism involves the intracellular sequestration of carboxyl-coordinated U(VI) into an insoluble complex with GSH, which is presumably related to the formation of U(VI)–GSSG or U(IV).

The interaction between short tripeptide like GSH and U is significant in the context of redox reaction, rather than due to its binding through one or two functional groups. Usually a longer peptide (>10 amino acids) is required to observe more specific binding patterns. The structural characteristics of calcium-binding proteins, particularly the EF-hand motif, have served as a model for the development of lanthanide-binding peptides, because of the similarity in the size of ionic radius of Ca^{2+} and Ln^{3+}. The binding of Ln^{3+} by calmodulin–peptide has been thoroughly studied,[82] Pu^{4+} interactions with two variants of calmodulin–peptide have been also studied,[66] and recently such study has been extended to lanmodulin peptides[83] and even those with the reversed sequences[84] (Fig. 7). So-called lanthanide-binding tags (LBT) with high and selective recognition of lanthanides are also known for more than 20 years,[85–87] which was later extended to Am^{3+}-binding research.[88] Jeanson and coauthors designed An(III) and An(IV) binding peptides from a "scratch" and made systematic investigation, though their strategy was primarily focused on utilizing acidic amino acids exclusively.[89,90]

Uranium (and thorium) is perhaps one of the most intensively studied elements among lanthanides and actinides for its binding with peptides,[91–95] due to their affordability and minimal radioactivity, which facilitates their handling in laboratory settings. However, these elements may not be the most intriguing for study in terms of recovery and separation because they are the most abundant actinide elements in nature. Conversely, their abundance in nature has led to significant research interest in their detection. The potential health implications of human exposure to uranium encompass both radiological and chemical toxicity.[96] The average U concentration in drinking water varies significantly among different regions and countries,[97,98] and the presence of U in aquifers has the potential to pose health concerns mainly because of its chemotoxicity. The development of its *in situ* measuring technique is awaited. The development of peptide-based sensors for U/Th detection has emerged as a prominent research area in recent years.[99–101] Phosphorylation of peptide is frequently employed to enhance their binding affinity to actinides.[102–105] However, this process transforms the peptide into a mere scaffold, prompting the question of whether the

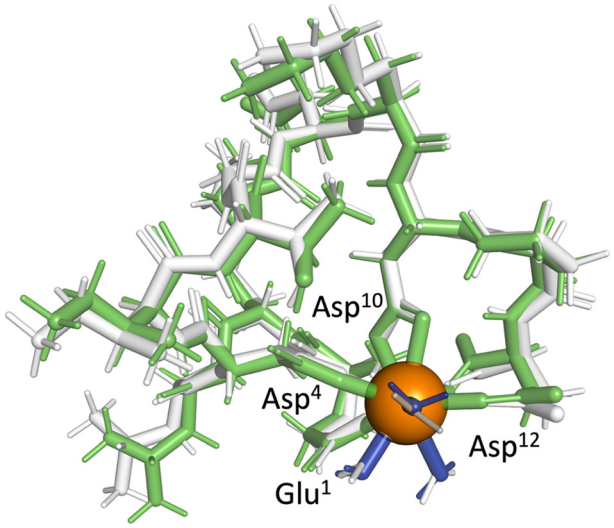

Fig. 7 The optimized structures of Eu^{3+}-bound reversed lanmodulin EF Hand 1 peptide obtained by DFT calculations with dispersion corrections and LC-ECP (six 4f electrons incorporated into the frozen core) applied on Eu^{3+}. Green sticks, orange ball, blue sticks depict the peptide, Eu^{3+}, three coordinating water molecules, respectively. Gray sticks show the previously-calculated structure[84] using MD simulations based on 12-6-4 LJ potential on Eu^{3+}. Two structures (DFT and MD) are superimposed to highlight their agreement.

use of noble materials like peptides is truly essential when their sole function is to serve as the backbone that hold the phosphoryl groups hands for the capture of metal ions. In an alternative approach, His-decorated phenanthroline diimide was utilized for the recovery of Am^{3+}.[106] In this instance, the incorporation of amino acids was intended to enhance solubility and they are not involved in metal-binding. Some prominent chelators, including DOTA (dodecane tetraacetic acid), EDTA (ethylenediaminetetraacetic acid), and NTA (nitrilotriacetic acid) are classified as aminopolycarboxylic acids. These chelators share Gly as a parental complex. The complexation of these chelators with trivalent actinides is a subject of intensive research in the direction of separation of lanthanides and minor actinides.[107]

Radiopharmaceuticals are also complexes that contain a peptide segment in their structure, as well as a separate metal-capturing chelator component. In the case of radiopharmaceuticals, however, the peptide portion plays a distinct role in binding with a receptor at its extracellular domain, thereby inducing a conformational change in the receptor and activating its intracellular domain. For the metal-capturing component, a strong chelator such as DOTA is typically selected. In recent years, a novel research domain has emerged that utilizes these chelators for radiotherapy. ^{225}Ac-based radiopharmaceuticals have gained increased attention for its application in α-particle therapy, a treatment modality that has been shown to be more effective in the destruction of tumour cells when compared to β-emitting radionuclides.[108] In this particular context, as well, phosphorylation has been identified as a promising strategy to enhance the binding affinity of Ac^{3+}.[109,110] It should be noted that the coordination chemistry of Ac^{3+} is still rather poorly understood,[111] and studies on its daughter products, such as Fr and At, are even more scarce. It is frequently assumed that Ac^{3+} persists in binding to the chelator subsequent to its decay to its daughters. However, this is exceedingly improbable, given that Fr^{+} is the largest cation in the periodic table. It is imperative that further investigation be conducted into the coordination chemistry of these elements (Ac, Fr, At), which have received the least attention in the periodic table so far.

Now, we will shift the discussion to an entirely different topic; the implementation of computer chemistry in this research domain. While the application of computer chemistry, such as density functional theory (DFT), has been extensively implemented in the field of general actinide chemistry, its application in the context of actinide interaction with peptide or protein has been extremely scarce. However, this emerging field has undergone significant development in the past decade, a topic which will be discussed in the remainder of this section. Due to smaller size of peptides in comparison to proteins, they offer greater potential for computer simulation, and the application of computational chemistry in this field is expected to become more widespread in the future. Quantum chemical calculations (*e.g.* DFT) and classical molecular dynamics (MD) simulations can be employed to study peptide structures and their metal bindings. Each method addresses different aspects and has different strengths. Quantum chemistry is an *ab initio* method that provides accurate electronic and geometric structures of peptides. In contrast, classical MD simulation is based on empirical parameters and is more suited for simulating dynamic behaviour and conformational changes of peptides. Peptides are known for their structural flexibility, which complicates the prediction of their structures, including those in metal-bound states. Peptide structure optimization frequently lacks any initial structures to begin with. In such cases, the use of DFT can prove challenging in terms of identifying the global energy minimum with reasonable computational cost. The employment of a more expeditious and dynamic approach, such as classical MD simulations, is often a more suitable alternative. There was great advent in this field in the last decade largely due to the parameterization of M^{3+} and M^{4+} ions using the 12-6-4 Lennard-Jones-type nonbonded model by the group of Kenneth Merz.[112–114] Their parametrization included exotic ions such as Th^{4+}, U^{4+}, and Pu^{4+}. The structures of Eu^{3+}-bound peptide obtained by using their 12-6-4-type potential is comparable to the DFT-optimized structure, which prove their validity (Fig. 7). Hay and coworkers extended this potential (parametrized for water coordination) to the protein system to better reproduce the binding energy for M^{3+}-binding peptides.[115] Not all MD programs are compatible with 12-6-4-type potentials, and the widely-used GROMACS software cannot handle this type of potentials, which is a significant setback to the research in this direction. In an another effort, the group of Stefan Grimme has recently extended robust atomistic

generic force field GFN-FF to lanthanide and actinide biomolecule system and claimed that the structures they obtained are almost comparable to those using DFT.[116] Another interesting and important development by Grimme and his coworkers is the development of composite methods which he calls "Swiss army knife" and utilizes relatively small basis sets and special corrections to achieve high accuracies at a fraction of the computational cost of a calculation approaching the basis set limit. In the realm of computational chemistry, intermediate methods that straddle the divide between quantum chemistry (*e.g.* DFT) and classical mechanics include the QM/MM approach and the FMO (fragment molecular orbital) method (Fig. 8). These methods possess two key advantages. Firstly, they are significantly less expensive than purely quantum chemistry-based methods. Secondly, they are more accurate in energetics than purely classical mechanics-based approaches. We have recently successfully applied FMO methods in various lanthanide/actinide-containing biological system with the help of group of Yuji Mochizuki.[25,117,118]

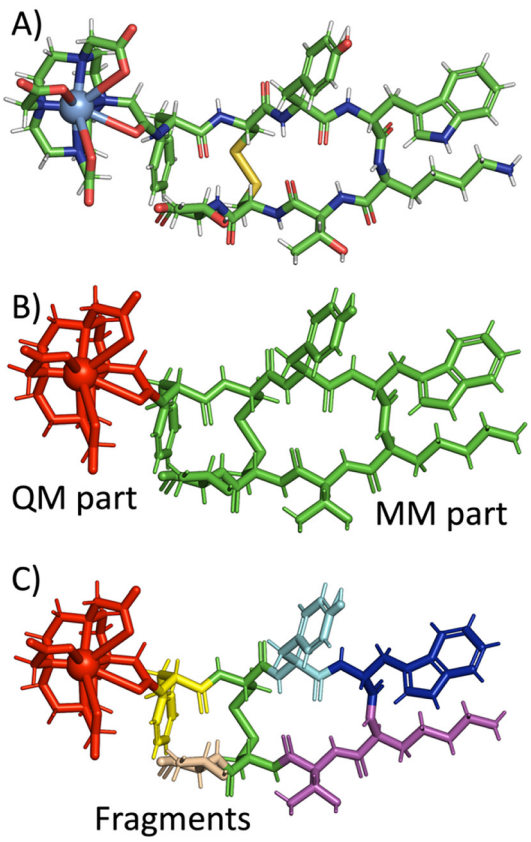

Fig. 8 Schematic illustration of different computational approaches. (A) Conventional methods (QM or MM) apply a single level of theory to the entire system. (B) QM/MM treats a key region (red) with QM, and the remainder (green) with MM. (C) Fragment Molecular Orbital (FMO) theory divides the system into fragments, calculating energy of each fragment and fragment pairs using QM to reconstitute the energetic of the whole system.

4. Actinide and protein

A preliminary analysis of the existing literatures on actinide/lanthanide interactions with protein reveals the presence of three predominant research categories. The initial category pertains to the utilization of proteins for the recovery and/or separation of these elements. The second type of research entails the investigation of the potential of actinide to interact with proteins relevant to humans, and the subsequent impact on human health, particularly in the context of accidental exposure (*e.g.* nuclear accident). The third category of research has emerged within the last decade. The focus of those studies is on the protein/bacteria present in nature that are capable of utilizing lanthanide or actinide in their enzymatic activities. These three types of research are interconnected and frequently refer to analogous types of proteins or domains. Nevertheless, we discuss these subtopics independently.

A number of attempts have been made to recover hexavalent uranium (UO_2^{2+}) using protein-based materials.[119–122] However, such technology remains ambitious for practical application considering the relatively low market price of uranium (merely ~10 times that of copper).[123] In practice, there are much more economic approaches for the recovery of uranium from seawater,[124–127] though their economic viability still remains suboptimal, necessitating ongoing technological development. Nevertheless, in scenarios where the primary objective is the recovery of Ln/An from wastewater to avert environmental contamination, cost considerations become a secondary issue, and protein-based materials eventually emerge as a viable alternative.[128,129] It also remains a significant challenge to separate Ln and An or amongst themselves, especially in the nuclear industry, for which protein-based materials could be utilized.[130,131] In the context of metal ion recovery and isolation from a matrix or from wastewater for the purpose of bioremediation, the utilization of abundant materials such as surface layer (S-layer) protein is advantageous due to the heterogeneity of these materials, which does not pose a significant problem.[128] On the other hand, in scenarios where the objective is mutual separation of metal ions, the homogeneity of the material becomes a central concern, necessitating the purification of the material. In general, peptide is more appropriate for such purpose rather than protein. This is because only few amino acid residues are anyway committed to metal-binding. Consequently, in the absence of a significant breakthrough in the research, such as the confirmation of bulk, biologically mass-producible proteins that are effective in the separation of actinides and/or lanthanides, further research in this area appears to be challenging. In this particular context, alcohol dehydrogenase (ADH) enzymes have been observed to exhibit the capacity to utilize lanthanides and actinides, and even demonstrate a degree of discrimination among them. This issue will be addressed subsequently in this section.

With regard to the interaction between actinide and protein in human-related scenarios, Creff *et al.*[132] provided an excellent comprehensive review on this topic, which summarizes

previous studies conducted since the Manhattan project. Creff *et al.* describe that primary tasks of previous researches can be classified into three categories; first the identifications of the proteins that are relevant to human-related scenarios, second the investigations on the structures and the affinities of the An-binding proteins, and third to study the impact of uptake of An-bound proteins. Serum proteins have been extensively employed to study its affinity to actinides, as they play crucial role in facilitating metal transportation within the human body, suggesting a potential for involvement in actinide transport processes. This includes studies of actinide interactions with albumin,[133] transferrin,[134–136] ferritin,[137,138] and hemoglobin.[139] The collective findings of these studies indicated high affinity between actinide and proteins, with the potential binding site of actinide being either specific or non-specific (Fig. 9). *In vivo* studies employing rats after implantation with depleted uranium fragments have demonstrated U accumulation in their kidneys and bones. However, the study also exhibited a minor increase in serum U levels, attributable to rapid urinary excretion.[140] Therefore it is important to note that while certain proteins possess a high capacity to incorporate actinides, this does not inherently signify that those proteins function as actinide accumulators within the human body. On the other hand, it has been hypothesized that the process of bone turnover involving Th(IV) and Pu(IV) is associated with the presence of hyperphosphorylated proteins, such as osteopontin.[141] Phosphorylated proteins are generally identified as strong actinide binders as in the case of phosvitin[142,143] and bovine milk protein.[144] This is also one of the reasons why phosphorylation is frequently used as a strategy to increase the affinity of peptides towards lanthanides and actinides, as we discussed in the preceding section. Another protein that has been extensively studied in relation to lanthanide and actinide binding is calmodulin, a calcium-binding messenger protein. It has been demonstrated that calmodulin can accommodate up to four Ln^{3+} (or An^{3+}) ions.[117] Cotruvo *et al.* have discovered calmodulin-like protein which has high selectivity for Ln^{3+} (and An^{3+}) and named it as lanmodulin.[7,145] However, the actinide–calmodulin interaction appears rather irrelevant in connection to human health issues, and its high affinity is discussed and utilized in a separate setting. Overall, there are still many open questions in this field of research. For instance, the genotoxicity of uranium has been demonstrated not to be necessarily associated with U–protein interaction. Rather, U genotoxicity has been suggested to be more associated with DNA strand breaks and chromosome aberrations.[96] The issue of actinide toxicity in the human body is not a simple problem that can be attributed to the interaction with several particular proteins. Further comprehensive research is needed to elucidate the mechanisms by which this toxicity occurs. At the same time, it is also imperative to have parallel studies on decorporation agents of actinides to prepare for accidental exposure of humans.[146–148]

The third category of research constitutes an emerging new field of science, which is concerned with the proteins (and enzymes) present in the nature that are capable of accommodating lanthanide or actinide ions. Trivalent lanthanides were long believed to lack any essential biological function. However, in 2011, Kawai and coauthors revealed the catalytic role of trivalent lanthanide ions in the enzyme methanol dehydrogenase (MDH).[6,149,150] Later, the growth of the *Methylacidiphilum fumariolicum* strain SolV, isolated from volcanic mud water in Italy, was found to be strictly dependent on the concentration of Ln^{3+} ions.[151] It was even confirmed that XoxF-type MDH can discriminate amongst different lanthanides.[152] In XoxF-type MDH, lanthanide binding to the cofactor pyrroloquinoline quinone (PQQ) was found to transition from a chelate to an unidentate conformation as the lanthanides transition from lighter to heavier elements. This observation was made through the use of molecular dynamics

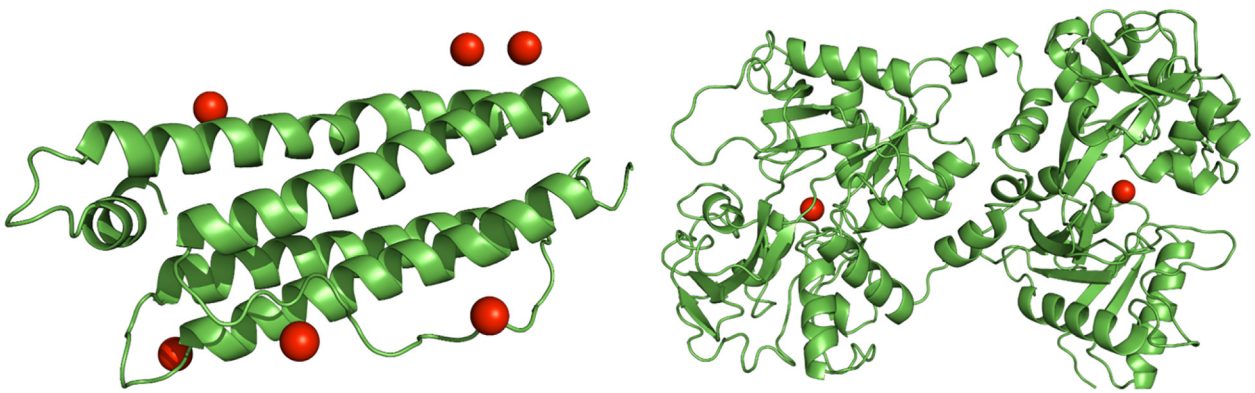

Fig. 9 The structures of plutonium(IV)-bound proteins from molecular dynamics (MD) simulations[136,137] based on 12-6-4-type Lennard-Jones potentials on Pu^{4+}. The left-hand side of the figure displays Pu^{4+}-bound ferritin, a single L chain of horse ferritin (PDB reference 1AEW) with six Pu^{4+} ions present. The right-hand sides of the figure displays Pu^{4+}-bound transferrin, a transferrin (PDB reference 1FCK) incorporating two Pu^{4+} ions. In both figures, protein structures are depicted as green ribbon and Pu^{4+} ions as red balls. Waters and other ions (Na^+, CO_3^{2-}, *etc.*) are omitted for clarity. Note that in the case of ferritin, Pu^{4+} ions are bound to the carboxylic groups of random acidic residues (Asp, Glu) in a non-specific manner, whereas in the case of transferrin two Pu^{4+} ions are stably accommodated in the iron-binding sites of transferrin with a closed conformation.

(MD) simulations.[118] The enzymatic activity exhibited by XoxF-type MDH, which is exclusive to lighter lanthanides, was identified as the underlying cause of this phenomenon (Fig. 10). These discoveries expanded the significance of Ln^{3+} ions in biochemistry and in bacterial metabolism. Recent findings have even confirmed that active microbial methanol oxidation in the ocean by MDH is almost entirely Ln-dependent despite the fact that Ln exist only in trace concentrations,[153] and that Ln–MDHs are far more broadly distributed than the Ca–MDHs. In the field of biology, it is common to observe examples where the life of organism is dependent on trace elements, and these elements become toxic at higher concentrations. The prevalence of Ln-dependent MDH in natural environments suggests the potential for a novel and hitherto unrecognized role for lanthanide (and potentially actinide as well) in a complexity that is both novel and hitherto unappreciated. In this context, the discovery of actinide-dependent MDH was not unexpected.[10] Consequently, the hypothesis that actinides played a certain role in the evolution of primitive metabolic processes (as we discussed in Introduction) may not be entirely dismissed. Despite that actinide-dependent MDH has been confirmed exclusively for heavy actinides Am(III) and Cm(III) in a laboratory setting, given the presence of a high H_2 concentration in the Hadean earth's atmosphere (some sources refer to this as large as ~0.1 bar), the possibility of Pu(III) being present, along with their association with MDH, remains a possibility. Indeed, it is hypothesized that Pu in Oklo (Gabon) from natural reactor in reaction zone 16 existed as Pu(III).[154] The isolation and identification of protein lanmodulin[7] revealed its capacity to utilize light to heavy actinides, including Ac(III),[155] Am(III) and Cm(III).[145,156–158] A recent study revealed that a specific type of lanmodulin from *Hansschlegelia quercus* exhibits sensitivity to the size of Ln^{3+}.[159] This finding is analogous to the discovery previously made for Ln-dependent MDH,[152] though in the case of MDH the effect of the size of Ln^{3+} ions appears more critically in their structures by switching the coordination mode of cofactor pyrroloquinoline quinone (PQQ) (Fig. 10). In comparison to its Ca^{2+}-binding counterpart calmodulin, lanmodulin exhibits a significantly shorter sequence, containing only half as many residues in its EF hand loop (12 or 13 for lanmodulin, whereas 24 or 25 for calmodulin). The results of evolutionary studies are awaited to ascertain whether these two proteins are genetically related and whether they have undergone an increase or decrease in size and complexity through processes such as gene duplication and fusion. Such study may provide preliminary evi-

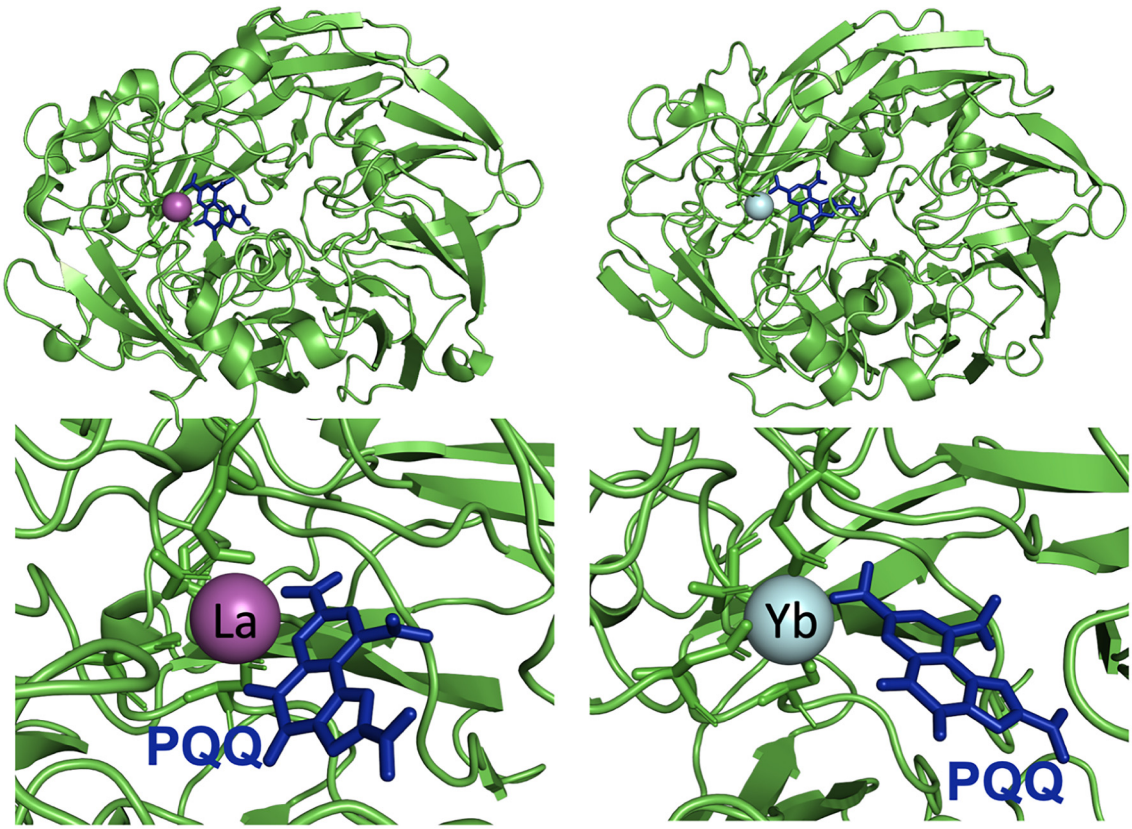

Fig. 10 The structures of La^{3+}- and Yb^{3+}-bound methanol dehydrogenase (MDH, XoxF-type) from molecular dynamics simulations.[118] On the left- and right-hand sides are La^{3+}- and Yb^{3+}-bound MDH, respectively. The top views show global conformation of the metalloenzyme whereas the bottom views show the central metal ion and its vicinity including cofactor pyrroloquinoline quinone (PQQ). Only in the La^{3+}-bound MDH, PQQ coordinates to metal ion in chelate binding mode thereby allowing nucleophilic attack of the methanol oxygen on PQQ.

dence that shorter Ln/An-bound proteins may have existed earlier in evolution than their Ca^{2+}-bound counterparts, and may lend further credit to the hypothesis that primitive proteins and enzymes have utilized Ln and/or An. A recently discovered lanthanide-binding protein, Lanpepsy, has been found to possess three to four binding sites for Ln^{3+} ions.[160] This finding provides further evidence for the prevalence of lanthanide-dependent life.

5. Summary and perspectives

This Perspective presents a comprehensive review of the interplay between actinides and biomolecules. A thorough review of actinide coordination chemistry reveals a complex landscape of interactions of actinides with carboxylates, amino acids, peptides, and proteins. The formation of stable oligomeric complexes, particularly the hexanuclear An^{4+} clusters, underscores the potential for actinides to influence their solubility, stability, and transport in the environment. The observed preference for *syn–syn* bridging carboxylates, in conjunction with the influence of hydrolysis on complex formation, suggests the existence of specific pathways for the assembly of more complex structures including AnO_2. A more extensive study of the potential transport route and the mechanism of An nanoparticles in the vicinity of a natural nuclear reactor are necessary to elucidate the roles of early actinides in primitive life. Such studies are also important in the context of nuclear waste disposal.

The emerging field of actinide-dependent proteins, as exemplified by lanthanide-dependent methanol dehydrogenase and lanmodulin, may supports the notion that lanthanides and actinides were not merely passive participants in early metabolic processes, but could have been actively incorporated into the catalytic role in early life. The discovery of these enzymes challenges the long-held assumption that life is exclusively reliant on a limited set of metal cofactors and opens the possibility that lanthanide (or actinide)-based metalloenzymes may have played a crucial role in the earliest stages of evolution. Further phylogenetic analyses are necessary to confirm that lanthanide (or actinide)-dependent enzymes possess in fact ancestral features and that the calcium-dependent versions evolved later, as discussed elsewhere.[161] The observation that some of these proteins exhibit selectivity for different lanthanides and even actinides, and that this selectivity is linked to their ionic radii and coordination preferences, underscores the potential for fine-tuning of metabolic pathways through subtle variations in metal composition. Additionally, there is little knowledge regarding the interactions between tetravalent actinide and proteins, despite the significance of this oxidation state in geologic implications (as exemplified by the formation of An^{4+} polymers). Addressing this knowledge gap is imperative.

Significant challenges remain in fully evaluating the validity of the nuclear geyser model. While we have presented a compelling case for the chemical feasibility of actinide-driven abiogenesis, direct evidence linking natural nuclear reactors to the origin of life remains elusive. Furthermore, the inherent complexity of prebiotic systems necessitates a multidisciplinary approach that integrates geochemistry, radiochemistry, biochemistry, and computational modelling. Ultimately, resolving the question of whether actinides played a significant role in the origin of life will require a sustained and collaborative effort involving researchers from diverse disciplines. Such investigations will not only provide a deeper understanding of the fundamental processes that gave rise to life on earth, but also a more informed approach to the high-level radioactive waste disposal in the geosphere.

Author contributions

S. T.: Conceptualization, investigation, funding acquisition, project administration, supervision, writing—original draft, writing—review and editing. K. T.: Conceptualization, investigation, funding acquisition, project administration, supervision, writing—original draft, writing—review and editing. All authors have read and agreed to the published version of the manuscript.

Conflicts of interest

There are no conflicts to declare.

Data availability

No primary research results, software or code have been included and no new data were generated or analysed as part of this review.

Acknowledgements

We thank all colleagues at SciTokyo, HZDR, and other associated institutes. This Perspective was supported in part by Grant-in-Aid for JSPS Fostering Joint International Research (B) (JP20KK0119), Grant-in-Aid for Scientific Research (B) (JP24K01398), and International Collaborative Research (JP24KK0109).

References

1 T. Ebisuzaki and S. Maruyama, Nuclear geyser model of the origin of life: Driving force to promote the synthesis of building blocks of life, *Geosci. Front.*, 2017, **8**(2), 275–298.
2 S. Maruyama, T. Ebisuzaki and K. Kurokawa, Review of the Nine Requirements for the Birthplace of Life and the Nuclear Geyser Model: The Only Possible Site for the Birthplace of Life on Hadean Earth, *J. Geogr.*, 2019, **128**(4), 513–548.

3 S. L. Miller, A Production of Amino Acids Under Possible Primitive Earth Conditions, *Science*, 1953, **117**, 528–529.
4 T. Ebisuzaki, H. Nishihara, K. Kurokawa, H. Mori, Y. Kamagata, H. Tamaki, R. Nakai, T. Oshima, M. Hara, T. Suzuki and S. Maruyama, Hadean Primordial Metabolism Pathway Driven by a Nuclear Geyser, *J. Geogr.*, 2020, **129**(6), 779–804.
5 Z. Adam, Actinides and Life's Origins, *Astrobiology*, 2007, **7**(6), 852–871.
6 Y. Hibi, K. Asai, H. Arafuka, M. Hamajima, T. Iwama and K. Kawai, Molecular structure of La^{3+}-induced methanol dehydrogenase-like protein in Methylobacterium radiotolerans, *J. Biosci. Bioeng.*, 2011, **111**(5), 547–549.
7 J. A. Cotruvo Jr., E. R. Featherston, J. A. Mattocks, J. V. Ho and T. N. Laremore, Lanmodulin: A Highly Selective Lanthanide-Binding Protein from a Lanthanide-Utilizing Bacterium, *J. Am. Chem. Soc.*, 2018, **140**(44), 15056–15061.
8 L. Daumann, Essential and Ubiquitous: The Emergence of Lanthanide Metallobiochemistry, *Angew. Chem., Int. Ed.*, 2019, **58**, 12795–12802.
9 J. A. Mattocks and J. A. Cotruvo Jr., Biological, biomolecular, and bio-inspired strategies for detection, extraction, and separations of lanthanides and actinides, *Chem. Soc. Rev.*, 2020, **49**, 8315–8334.
10 H. Singer, R. Steudtner, A. S. Klein, C. Rulofs, C. Zeymer, B. Drobot, A. Pol, N. C. Martinez-Gomez, H. J. M. Op den Camp and L. J. Daumann, Minor Actinides Can Replace Essential Lanthanides in Bacterial Life, *Angew. Chem., Int. Ed.*, 2023, **62**(31), e202303669.
11 J. J. Woods, N. M. Good, A. G. Cosby, K. Wadhawan, J. N. Wacker, A. N. Gaiser, N. C. Martinez-Gomez and R. J. Abergel, Expanding on the ability of trivalent actinides to support microbial alcohol metabolism in evolved methylotrophic bacterium, *Commun. Chem.*, 2025, **8**, 367.
12 Y. Sawaki, T. Sato, W. Fujisaki, H. Ueda, H. Asanuma and S. Maruyama, Geology around Natural Reactors and Birthplace of Eukaryotes, *J. Geogr.*, 2019, **128**(4), 549–569.
13 T. Takeyama, S. Tsushima, R. Gericke, T. M. Duckworth, P. Kaden, J. März and K. Takao, A Series of $AnVIO_2^{2+}$ Complexes (An= U, Np, Pu) with N_3O_2-Donating Schiff-Base Ligands: Systematic Trends in the Molecular Structures and Redox Behavior, *Inorg. Chem.*, 2025, **64**(3), 1313–1322.
14 G. J.-P. Deblonde, Biogeochemistry of Actinides: Recent Progress and Perspective, *ACS Environ. Au*, 2024, **4**(6), 292–306.
15 U. Casellato, P. A. Vigato and M. Vidali, Actinide Complexes with Carboxylic Acids, *Coord. Chem. Rev.*, 1978, **26**, 85–159.
16 A. Günther, G. Geipel and G. Bernhard, Complex formation of uranium(VI) with the amino acids L-glycine and L-cysteine: A fluorescence emission and UV–Vis absorption study, *Polyhedron*, 2007, **26**(1), 59–65.
17 A. Günther, G. Geipel and G. Bernhard, Complex formation of U(VI) with the amino acid L-threonine and the corresponding phosphate ester O-phospho-L-threonine, *Radiochim. Acta*, 2006, **94**, 845–851.
18 W. Xie, A. Badawi, H. Huang and J. D. Van Horn, Solution interactions between the uranyl cation $[UO_2^{2+}]$ and histidine, N-acetyl-histidine, tyrosine, and N-acetyl-tyrosine, *J. Inorg. Biochem.*, 2009, **103**, 58–63.
19 P. Thuéry, Y. Atoini and J. Harrowfield, Functionalized Aromatic Dicarboxylate Ligands in Uranyl–Organic Assemblies: The Cases of Carboxycinnamate and 1,2-/1,3-Phenylenedioxydiacetate, *Inorg. Chem.*, 2020, **59**(5), 2923–2936.
20 J. D. Van Horn and H. Huang, Uranium(VI) bio-coordination chemistry from biochemical, solution and protein structural data, *Coord. Chem. Rev.*, 2006, **250**, 765–775.
21 Y. W. Lin, Uranyl Binding to Proteins and Structural-Functional Impacts, *Biomolecules*, 2020, **10**(3), 457.
22 A. F. Lucena, L. Maria, J. K. Gibson and J. Marçalo, Examining Interactions of Uranyl(VI) Ions with Amino Acids in the Gas Phase, *Appl. Sci.*, 2023, **13**, 3834.
23 J. de Groot, B. Cassell, M. Basile, T. Fetrow and T. Z. Forbes, Charge-Assisted Hydrogen-Bonding and Crystallization Effects within UVI Glycine Compounds, *Eur. J. Inorg. Chem.*, 2017, **13**, 1938–1946.
24 M. R. Duff and C. V. Kumar, Site-Selective Photocleavage of Proteins by Uranyl Ions, *Angew. Chem., Int. Ed.*, 2006, **45**, 137–139.
25 S. Tsushima, J. Kretzschmar, H. Doi, K. Okuwaki, M. Kaneko, Y. Mochizuki and K. Takao, Towards tailoring hydrophobic interaction with uranyl(vi) oxygen for C–H activation, *Chem. Commun.*, 2024, **60**, 4769–4772.
26 Z. Szabó and I. Grenthe, Potentiometric and Multinuclear NMR study of the Binary and Ternary Uranium(VI)-L-Fluoride Systems, Where L Is α-Hydroxycarboxylate or Glicine, *Inorg. Chem.*, 2000, **39**, 5036–5043.
27 N. W. Alcock, D. J. Flanders, T. J. Kemp and M. A. Shand, Glycine Complexation with Uranyl Ion: Absorptiometric, Luminescence, and X-Ray Srtuctural Studies of Tetrakis (glycine)dioxouranium(VI) Nitrate, *J. Chem. Soc., Dalton Trans.*, 1985, **3**, 517–521.
28 A. D. Keramidas, M. P. Rikkou, C. Drouza, C. P. R. Aptopoulou, A. Terzis and I. Pashalidis, Investigation on uranyl interaction with bioactive ligands. Synthesis and structural studies of the uranyl complexes with glycine and N-(2-mercaptopropionyl)glycine, *Radiochim. Acta*, 2002, **90**, 549–554.
29 P. A. Smith, T. L. Spano and P. C. Burns, Synthesis and structural characterization of a series of uranyl-betaine coordination complexes, *Z. Kristallogr.*, 2018, **233**(7), 507–513.
30 G. Bombieri, E. Forsellini, G. Tomat and L. Magon, Structural Studies on the Actinide Carboxylates. II. The Crystal and Molecular Structure of Bis(iminodiacetato) dioxouranium(VI), *Acta Crystallogr., Sect. B*, 1974, **30**, 2659–2663.
31 G. A. Battiston, G. Sbrignadello, G. Bandoli, D. A. Clemente and G. Tomat, Synthesis and

Characterization of some Actinoid Iminodiacetato-complexes: Crystal Structure and Normal Co-ordinate Analysis of Iminodiacetatodioxouranium(VI), *J. Chem. Soc., Dalton Trans.*, 1979, **12**, 1965–1971.

32 J. Jiang, M. J. Sarsfield, J. C. Renshaw, F. R. Livens, D. Collison, J. M. Charnock, M. Helliwell and H. Eccles, Synthesis and Characterization of Uranyl Compounds with Iminodiacetate and Oxydiacetate Displaying Variable Denticity, *Inorg. Chem.*, 2002, **41**, 2799–2806.

33 Y. Atoini, J. Harrowfield, Y. Kim and P. Thuéry, Filling the equatorial garland of uranyl ion: its content and limitations, *J. Inclusion Phenom. Macrocyclic Chem.*, 2021, **100**, 89–98.

34 S. Panchanan, R. Hämäläinen and P. S. Roy, Synthesis, Chiroptical and Electrochemical Studies of Dioxouranium (VI) Complexes of Aldimine Derivatives of L-/D- Histidine and Crystal Structure of (2,2′-Bipyridyl)dioxo-(N-o-vanillylidene-L- histidinato)uranium(VI)-Water-Methanol(1/1/1), *J. Chem. Soc., Dalton Trans.*, 1994, **16**, 2381–2390.

35 J. de Groot, K. Gojdas, D. K. Unruh and T. Z. Forbes, *Cryst. Growth Des.*, 2014, **14**, 1357–1365.

36 X.-T. Xu, Y.-N. Hou, S.-Y. Wei, X.-X. Zhang, F.-Y. Bai, L.-X. Sun, Z. Shi and Y.-H. Xing, UO_2^{2+}-amino hybrid materials: structural variation and photocatalysis properties, *CrystEngComm*, 2015, **17**, 642–652.

37 M. T. Weller, M. E. Light and T. Gelbrich, Structure of uranium(VI) oxide dihydrate, $UO_3{\cdot}2H_2O$; synthetic metaschoepite $(UO_2)_4O(OH)_6{\cdot}5H_2O$, *Acta Crystallogr., Sect. B: Struct. Sci.*, 2000, **56**, 577–583.

38 K. E. Knope and L. Soderholm, Solution and Solid-State Structural Chemistry of Actinide Hydrates and Their Hydrolysis and Condensation Products, *Chem. Rev.*, 2013, **113**(2), 944–994.

39 R. Weinland and A. Stark, Über Komplexe der Ameisensäure mit Thorium. Anhang: Über ein Aluminium- und ein Manganiformiat, *Ber. Dtsch. Chem. Ges. A, B*, 1926, **59**(3), 471–479.

40 H. Reihlen and M. Debus, Über Thoriumformiate, *Z. Anorg. Allg. Chem.*, 1929, **178**(1), 157–176.

41 S. Takao, K. Takao, W. Kraus, F. Emmerling, A. C. Scheinost, G. Bernhard and C. Hennig, First Hexanuclear UIV and ThIV Formate Complexes – Structure and Stability Range in Aqueous Solution, *Eur. J. Inorg. Chem.*, 2009, 4771–4775.

42 L. M. Mokry, N. S. Dean and C. J. Carrano, Synthesis and Structure of a Discrete Hexamer Uranium-Phosphate Complex, *Angew. Chem., Int. Ed. Engl.*, 1996, **35**, 1497–1498.

43 J.-C. Berthet, P. Thuéry and M. Ephritikhine, Unprecedented reduction of the uranyl ion $[UO_2]^{2+}$ into a polyoxo uranium(IV) cluster: Synthesis and crystal structure of the first f-element oxide with a $M_6(\mu_3\text{-}O)_8$ core, *Chem. Commun.*, 2005, 3415–3417.

44 V. Mougel, B. Biswas, J. Pécaut and M. Mazzanti, New insights into the acid mediated disproportionation of pentavalent uranyl, *Chem. Commun.*, 2010, **46**, 8648–8650.

45 K. E. Knope, R. E. Wilson, M. Vasiliu, D. A. Dixon and L. Soderholm, Thorium(IV) Molecular Clusters with a Hexanuclear Th Core, *Inorg. Chem.*, 2011, **50**, 9696–9704.

46 K. Takao, S. Takao, A. C. Scheinost, G. Bernhard and C. Hennig, Formation of Soluble Neptunium(IV) Nanoclusters in Aqueous Solution: Growth Termination of Actinide(IV) Hydrous Oxides by Carboxylates, *Inorg. Chem.*, 2012, **51**, 1336–1344.

47 R. D. Shannon, Revised effective ionic radii and systematic studies of interatomic distances in halides and chalcogenides, *Acta Crystallogr., Sect. A*, 1976, **32**, 751–767.

48 K. E. Knope and L. Soderholm, Plutonium(IV) cluster with a hexanuclear $[Pu_6(OH)_4O_4]^{12+}$ core, *Inorg. Chem.*, 2013, **52**(12), 6770–6772.

49 C. Tamain, T. Dumas, D. Guillaumont, C. Hennig and P. Guilbaud, First Evidence of a Water-Soluble Plutonium(VI) Hexanuclear Cluster, *Eur. J. Inorg. Chem.*, 2016, 3536–3540.

50 T. L. McCusker, N. A. Vanagas, J. E. S. Szymanowski, R. G. Surbella III, J. A. Bertke, A. Arteaga and K. E. Knope, Elucidating trends in synthesis and structural periodicity in a series of tetravalent actinide-oxo hexamers, *CrystEngComm*, 2025, **27**, 507–515.

51 G. Chupin, C. Tamain, T. Dumas, P. L. Solari, P. Moisy and D. Guilaumont, Characterization of a Hexanuclear Plutonium(IV) Nanostructure in an Acetate Solution via Visible–Near Infrared Absorption Spectroscopy, Extended X ray Absorption Fine Structure Spectroscopy, and Density Functional Theory, *Inorg. Chem.*, 2022, **61**(12), 4806–4817.

52 T. Loiseau, I. Mihalcea, N. Henry and C. Volkringer, The crystal chemistry of uranium carboxylates, *Coord. Chem. Rev.*, 2014, **266–267**, 69–109.

53 C. R. Martin, G. A. Leith and N. B. Shustova, Beyond structural motifs: the frontier of actinide containing metal–organic frameworks, *Chem. Sci.*, 2021, **12**, 7214–7230.

54 K. Lv, S. Fichter, M. Gu, J. März and M. Schmidt, An updated status and trends in actinide metal-organic frameworks (An-MOFs): From synthesis to application, *Coord. Chem. Rev.*, 2021, **446**, 214011.

55 E. A. Hiti, G. Bolla and R. D. Rogers, Crystallographic Evidence for Formation of M_6O_8/M_6O_9 f-Element Clusters in Hydrolysis Reactions, *Cryst. Growth Des.*, 2025, **25**, 2267–2324.

56 A. R. U. Parambil, J. P. Mathew, M. J. Parammal and J. De Roo, M_6O_8 metal oxo clusters: A key structural motif across the periodic table, *Coord. Chem. Rev.*, 2026, **546**, 216967.

57 C. Hennig, S. Takao, K. Takao, S. Weiss, W. Kraus, F. Emmerling and A. C. Scheinost, Structure and stability range of a hexanuclear Th(IV)-glycine complex, *Dalton Trans.*, 2012, **41**, 12818–12823.

58 Y.-J. Hu, K. E. Knope, S. Skanthakumar and L. Soderholm, Understanding the Ligand-Directed Assembly of a Hexanuclear ThIV Molecular Cluster in Aqueous Solution, *Eur. J. Inorg. Chem.*, 2013, 4159–4163.

59 C. Falaise, H. A. Neal and M. Nyman, U(IV) Aqueous Speciation from the Monomer to UO_2 Nanoparticles: Two

Levels of Control from Zwitterionic Glycine Ligands, *Inorg. Chem.*, 2017, **56**(11), 6591–6598.

60 L. Pan, R. Heddy, J. Li, C. Zheng, X.-Y. Huang, X. Tang and L. Kilpatrick, Synthesis and Structural Determination of a Hexanuclear Zirconium Glycine Compound Formed in Aqueous Solution, *Inorg. Chem.*, 2008, **47**, 5537–5539.

61 I. Pappas, M. Fitzgerald, X.-Y. Huang, J. Li and L. Pan, Thermally Resolved in Situ Dynamic Light Scattering Studies of Zirconium(IV) Complex Formation, *Cryst. Growth Des.*, 2009, **9**, 5213–5219.

62 M. Matsuoka, S. Tsushima and K. Takao, Fluorite-like hydrolyzed hexanuclear coordination clusters of Zr(IV) and Hf(IV) with syn-syn bridging N,N,N-trimethylglycine in soft crystal structures exhibiting cold-crystallization, *Inorg. Chim. Acta*, 2021, **528**, 120622.

63 C. Tamain, T. Dumas, C. Hennig and P. Guilbaud, Coordination of Tetravalent Actinides (An = ThIV, UIV, NpIV, PuIV) with DOTA: From Dimers to Hexamers, *Chem. – Eur. J.*, 2017, **23**, 6864–6875.

64 I. Grenthe, X. Gaona, A. V. Plyasunov, L. Rao, W. H. Runde, B. Grambow, R. J. M. Konings, A. L. Smith and E. E. Moore, *Second Update on the Chemical Thermodynamics of Uranium, Neptunium, Plutonium, Americium and Technetium*, OECD-NEA, Boulogne-Billancourt, France, 2020.

65 T. Mori, K. Takao and Y. Ikeda, Synthesis and Physical Properties of Novel Betainium-type Ionic Liquids Derived from Amino Acids, *Chem. Lett.*, 2015, **45**, 164–166.

66 L. Daronnat, V. Holfeltz, N. Boubals, T. Dumas, P. Guilbaud, D. M. Martinez, P. Moisy, S. Sauge-Merle, D. Lemaire, P. L. Solari, L. Berthon and C. Berthomieu, Investigation of the Plutonium(IV) Interactions with Two Variants of the EF-Hand Ca-Binding Site I of Calmodulin, *Inorg. Chem.*, 2023, **62**(21), 8334–8346.

67 V. Neck and J. I. Kim, Solubility and hydrolysis of tetravalent actinides, *Radiochim. Acta*, 2001, **89**, 1–16.

68 M. Cot-Auriol, M. Virot, T. Dumas, O. Diat, D. Menut, P. Moisy and S. I. Nikitenko, First observation of $[Pu_6(OH)_4O_4]^{12+}$ cluster during the hydrolytic formation of PuO_2 nanoparticles using H/D/kinetic isotope effect, *Chem. Commun.*, 2022, **58**, 13147.

69 G. E. Sigmon and A. E. Hixon, Extension of the Plutonium Oxide Nanocluster Family to Include $\{Pu_{16}\}$ and $\{Pu_{22}\}$, *Chem. – Eur. J.*, 2019, **25**(10), 2463–2466.

70 L. Soderholm, P. M. Almond, S. Skanthakumar, R. E. Wilson and P. C. Burns, The Structure of the Plutonium Oxide Nanocluster $[Pu_{38}O_{56}Cl_{54}(H_2O)_8]^{14-}$, *Angew. Chem., Int. Ed.*, 2007, **47**(2), 298–302.

71 R. E. Wilson, S. Skanthakumar and L. Soderholm, Separation of Plutonium Oxide Nanoparticles and Colloids, *Angew. Chem., Int. Ed.*, 2011, **50**(47), 11234–11237.

72 M. Cot-Auriol, S. Dourdain, T. Dumas, C. Tamain, D. Menut, M. O. J. Y. Hunault, P. L. Solari, P. Moisy, S. I. Nikitenko and M. Virot, Capturing the Elusive: A Snapshot of the Pu(IV) Hexanuclear Cluster Intermediate in the birth of PuO_2 Colloidal Nanoparticles, *Inorg. Chem.*, 2025, **64**(34), 17178–17188.

73 C. Falaise, C. Volkringer, J.-F. Vigier, A. Beaurain, P. Roussel, P. Rabu and T. Loiseau, Isolation of the Large {Actinide}38 Poly-oxo Cluster with Uranium, *J. Am. Chem. Soc.*, 2013, **135**, 15678–15681.

74 L. Chatelain, R. Faizova, F. Fadaei-Tirani, J. Péaut and M. Mazzanti, Structural Snapshots of Cluster Growth from $\{U_6\}$ to $\{U_{38}\}$ During the Hydrolysis of UCl_4, *Angew. Chem., Int. Ed.*, 2019, **58**, 3021–3026.

75 A. Y. Romanchuk, I. E. Vlasova and S. N. Kalmykov, Speciation of Uranium and Plutonium From Nuclear Legacy Sites to Environment: A Mini Review, *Front. Chem.*, 2020, **8**, 630.

76 A. B. Kersting, D. W. Efurd, D. L. Finnegan, D. J. Rokop, D. K. Smith and J. L. Thompson, Migration of plutonium in ground water at the Nevada Test Site, *Nature*, 1999, **397**, 56–59.

77 R. Ono, T. Takeyama, R. Gericke, J. März, H. Kazama, T. Duckworth, S. Tsushima and K. Takao, Molecular and Crystal Structures of Pu(IV) Nitrato-Complexes Crystallized with Double-Headed 2-Pyrrolidone Derivatives and Systematic Trends in Tetravalent f-Block Metals, *Inorg. Chem.*, 2025, **64**(31), 15825–15834.

78 H. C. Freeman, G. Robinson and J. C. Schoone, Crystallographic Studies of Metal-Peptide Complexes. I. Glycylglycylglicinocopper(II) Chloride Sesquihydrate, *Acta Crystallogr.*, 1964, **17**, 719–730.

79 J. Kretzschmar, T. Haubitz, R. Hübner, S. Weiss, R. Husar, V. Brendler and T. Stumpf, Network-like arrangement of mixed-valence uranium oxide nanoparticles after glutathione-induced reduction of uranium(VI), *Chem. Commun.*, 2018, **54**(63), 8697–8700.

80 M. Obeid, J. Oertel, M. Solioz and K. Fahmy, Mechanism of Attenuation of Uranyl Toxicity by Glutathione in Lactococcus lactis, *Appl. Environ. Microbiol.*, 2016, **82**(12), 3563–3571.

81 J. Kretzschmar, A. Strobel, T. Haubitz, B. Drobot, R. Steudtner, A. Barkleit, V. Brendler and T. Stumpf, Uranium(VI) Complexes of Glutathione Disulfide Forming in Aqueous Solution, *Inorg. Chem.*, 2020, **59**(7), 4244–4254.

82 L. Le Clainche, G. Plancque, B. Amekraz, C. Moulin, C. Pradines-Lecomte, G. Peltier and C. Vita, Engineering new metal specificity in EF-Hand peptides, *J. Biol. Inorg. Chem.*, 2003, **8**, 334–340.

83 S. M. Gutenthaler, S. Tsushima, R. Steudtner, M. Gailer, A. Hoffmann-Röder, B. Drobot and L. J. Daumann, Lanmodulin peptides – unravelling the binding of the EF-Hand loop sequences stripped from the structural corset, *Inorg. Chem. Front.*, 2022, **9**(16), 4009–4021.

84 S. M. Gutenthaler, J. Kretzschmar, S. Tsushima, R. Steudtner, B. Drobot and L. J. Daumann, Reversing Lanmodulin's Metal-binding Sequence in Uncapped Short Peptides Surprisingly Increases the Lanthanide Affinity, *Angew. Chem., Int. Ed.*, 2025, **64**(46), e202510453.

85 M. Nitz, K. J. Franz, R. L. Maglathlin and B. Imperiali, A Powerful Combinational Screen to Identify High-Affinity Terbium(III)-binding Peptides, *ChemBioChem*, 2003, **4**, 272–276.
86 T. Hatanaka, N. Kikkawa, A. Matsugami, Y. Hosokawa, F. Hayashi and N. Ishida, The origins of binding specificity of a lanthanide ion binding peptide, *Sci. Rep.*, 2020, **10**, 19468.
87 V. Mishra, M. Sundararajan, A. K. Pathak, P. D. Sawant and T. Bandyopadhyay, Tuning the lanthanide binding tags for preferential actinide chelation: an all atom molecular dynamics study, *Phys. Chem. Chem. Phys.*, 2025, **27**(6), 3486–3495.
88 S. Özçubukçu, K. Mandal, S. Wegner, M. P. Jensen and C. He, Selective recognition of americium by peptide-based reagents, *Inorg. Chem.*, 2011, **50**(17), 7937–7939.
89 A. Jeanson, *Interaction of actinides with amino acids: from peptides to proteins*, Universite Paris XI Orsay, France, 2008. https://inis.iaea.org/records/fhtcr-bdf78.
90 A. Jeanson, C. Berthon, S. Coantic, C. Den Auwer, N. Floquet, H. Funke, D. Guillaneux, C. Hennig, J. Martinez, P. Moisy, S. Petit, O. Proux, E. Quémeneur, P. L. Solari and G. Subra, The role of aspartyl-rich pentapeptides in comparative complexation of actinide(IV) and iron(III). Part 1, *New J. Chem.*, 2009, **33**, 976–985.
91 R. Pardoux, S. Sauge-Merle, D. Lemaire, P. Delangle, L. Guilloreau, J. M. Adriano and C. Berthomieu, Modulating uranium binding affinity in engineered calmodulin EF-hand peptides: effect of phosphorylation, *PLoS One*, 2012, **7**(8), e41922.
92 C. Lebrun, M. Starck, V. Gathu, Y. Chenavier and P. Delangle, Engineering Short Peptide Sequences for Uranyl Binding, *Chem. – Eur. J.*, 2014, **20**, 16566–16573.
93 S. Safi, A. Jeanson, J. Roques, P. L. Solari, F. Charnay-Pouget, C. Den Auwer, G. Creff, D. J. Aitken and E. Simoni, Thermodynamic and Structural Investigation of Synthetic Actinide–Peptide Scaffolds, *Inorg. Chem.*, 2016, **55**(2), 877–886.
94 Y. Gao, Q. Zhang, Y. Lv, S. Wang, M. Men, H. Kobayashi, Z. Xu and Y. Wang, Peptide–carbon hybrid membranes for highly efficient and selective extraction of actinides from rare earth elements, *J. Mater. Chem. A*, 2021, **9**, 14422–14431.
95 F. Laporte, Y. Chenavier, A. Botz, C. Gateau, C. Lebrun, S. Hostachy, C. Vidaud and P. Delangle, A Simple Fluorescence Affinity Assay to Decipher Uranyl-Binding to Native Proteins, *Angew. Chem., Int. Ed.*, 2022, **61**(26), e202203198.
96 A. Rossberg, T. Abe, K. Okuwaki, A. Barkleit, K. Fukuzawa, T. Nakano, Y. Mochizuki and S. Tsushima, Destabilization of DNA through interstrand crossing by UO_2^{2+}, *Chem. Commun.*, 2019, **55**, 2015–2018.
97 B. Flem, C. Reimann, K. Fabian, M. Birke, P. Filzmoser and D. Banks, Graphical statistics to explore the natural and anthropoegenic processes influencing the inorganic quality of drinking water, ground water and surface water, *Appl. Geochem.*, 2018, **88**, 133–148.
98 H. S. Virk, Comments on "Uranium standards in drinking water: an examination from scientific and socio-economic point of India", *Environ. Sci. Pollut. Res.*, 2024, **31**, 65169–65170.
99 G. M. Roozbahani, X. Chen, Y. Zhang, R. Xie, R. Ma, D. Li, H. Li and X. Guan, Peptide-Mediated Nanopore Detection of Uranyl Ions in Aqueous Media, *ACS Sens.*, 2017, **2**, 703–709.
100 G. M. Roozbahani, X. Chen, Y. Zhang, O. Juarez, D. Li and X. Guan, Computation-Assisted Nanopore Detection of Thorium Ions, *Anal. Chem.*, 2018, **90**, 5938–5944.
101 C. C. Thompson and R. Y. Lai, Threonine Phosphorylation of an Electrochemical Peptide-Based Sensor to Achieve Improved Uranyl Ion Binding Affinity, *Biosensors*, 2022, **12**, 961.
102 M. Starck, N. Sisommay, F. A. Laporte, S. Oros, C. Lebrun and P. Delangle, Preorganized Peptide Scaffolds as Mimics of Phosphorylated Proteins Binding Sites with a High Affinity for Uranyl, *Inorg. Chem.*, 2015, **54**(23), 11557–11562.
103 Q.-Y. Wu, F.-W. Zhai, W. Liu, L.-Y. Yuan, Z.-F. Chai and W.-Q. Shi, Interactions between uranium(VI) and phosphopeptide: experimental and theoretical investigations, *Dalton Trans.*, 2016, **45**(38), 14988–14997.
104 M. Starck, F. A. Laporte, S. Oros, N. Sisommay, V. Gathu, P. L. Solari, G. Creff, J. Roques, C. Den Auwer, C. Lebrun and P. Delangle, Cyclic Phosphopeptides to Rationalize the Role of Phosphoamino Acids in Uranyl Binding to Biological Targets, *Chem. – Eur. J.*, 2017, **23**, 5281.
105 L. Abou-Zeid, A. Pell, M. A. Saraiva, P. Deangle and C. Bresson, Hydropilic interaction liquid chromatography: An efficient tool for assessing thorium interaction with phosphorylated biomimetic peptides, *J. Chromatogr. A*, 2024, **1735**, 465341.
106 B. Li, L. Wang, Y. Kang, H. Cao, Y. Liu, Q. He, Z. Li, X. Tang, J. Chen, L. Wang and C. Xu, Amino Acid Decorated Phenanthroline Diimide as Sustainable Hydrophilic Am(III) Masking Agent with High Acid Resistance, *JACS Au*, 2024, **4**(9), 3668–3678.
107 C. D. Pilgrim, T. S. Grimes, C. Smith, C. R. Heathman, J. Mathew, S. Jansone-Popova, S. Roy, D. Ray, V. S. Bryantsev and P. R. Zalupski, Tuning aminopolycarboxylate chelators for efficient complexation of trivalent actinides, *Sci. Rep.*, 2023, **13**, 17855.
108 C. Kratochwil, F. Bruchertseifer, F. L. Giesel, M. Weis, F. A. Verburg, F. Mottaghy, K. Kopka, C. Apostolidis, U. Haberkorn and A. Morgenstern, 225Ac-PSMA-617 for PSMA-Targeted α-Radiation Therapy of Metastatic Castration-Resistant Prostate Cancer, *J. Nucl. Med.*, 2016, **57**, 1941–1944.
109 B. W. Stein, A. Morgenstern, E. R. Batista, E. R. Birnbaum, S. E. Bone, S. K. Cary, M. G. Ferrier, K. D. John, J. L. Pacheco, S. A. Kozimor, V. Mocko, B. L. Scott and P. Yang, *J. Am. Chem. Soc.*, 2019, **141**, 19404–19414.
110 A. Morgenstern, L. M. Lilley, B. W. Stein, S. A. Kozimor, E. R. Batista and P. Yang, Computer-aAssisted Design of

Macrocyclic Chelators for Actinium-225 Radiotherapeutics, *Inorg. Chem.*, 2021, **60**, 623–632.
111 G. J.-P. Deblonde, M. Zavarin and A. B. Kersting, The coordination properties and ionic radius of actinium: A 120-year-old enigma, *Coord. Chem. Rev.*, 2021, **446**(1), 214130.
112 P. Li and K. M. Merz, Taking into Account the Ion-Induced Dipole Interaction in the Nonbonded Model of Ions, *J. Chem. Theory Comput.*, 2014, **10**(1), 289–297.
113 P. Li, L. F. Song and K. M. Merz Jr., Parametrization of Highly Charged Metal Ions Using the 12–6–4 LJ-Type Nonbonded Model in Explicit Water, *J. Phys. Chem. B*, 2015, **119**, 883–895.
114 Z. Li, L. F. Song, P. Li and K. M. Merz, Parametrization of Trivalent and Tetravalent Metal Ions for the OPC3, OPC, TIP3P-FB, and TIP4P-FB Water Models, *J. Chem. Theory Comput.*, 2021, **17**(4), 2342–2354.
115 P. Kantakevicius, C. Mathiah, L. O. Johannissen and S. Hay, Chelator-Based Parameterization of the 12–6–4 Lennard-Jones Molecular Mechanics Potential for More Realistic Metal Ion–Protein Interactions, *J. Chem. Theory Comput.*, 2022, **18**, 2367–2374.
116 T. Rose, M. Bursch, J.-M. Mewes and S. Grimme, Fast and Robust Modeling of Lanthanide and Actinide Complexes, Biomolecules, and Molecular Crystals with the Extended GFN-FF Model, *Inorg. Chem.*, 2024, **63**, 19364–19374.
117 B. Drobot, M. Schmidt, Y. Mochizuki, T. Abe, K. Okuwaki, F. Brulfert, S. Falke, S. A. Samsonov, Y. Komeiji, C. Betzel, T. Stumpf, J. Raff and S. Tsushima, Cm^{3+}/Eu^{3+} induced structural, mechanistic and functional implications for calmodulin, *Phys. Chem. Chem. Phys.*, 2019, **21**, 21213–21222.
118 S. Tsushima, Lanthanide-induced conformational change of methanol dehydrogenase involving coordination change of cofactor pyrroloquinoline quinone, *Phys. Chem. Chem. Phys.*, 2019, **21**, 21979–21983.
119 S. V. Wegner, H. Boyaci, H. Chen, M. P. Jensen and C. He, Engineering a uranyl-specific binding protein from NikR, *Angew. Chem., Int. Ed.*, 2009, **48**(13), 2339–2341.
120 L. Zhou, M. Bosscher, C. Zhang, S. Ozçubukçu, L. Zhang, W. Zhang, C. J. Li, J. Liu, M. P. Jensen, L. Lai and C. He, A protein engineered to bind uranyl selectively and with femtomolar affinity, *Nat. Chem.*, 2014, **6**(3), 236–241.
121 S. O. Odoh, G. D. Bondarevsky, J. Karpus, Q. Cui, C. He, R. Spezia and L. Gagliardi, UO_2^{2+} uptake by proteins: understanding the binding features of the super uranyl binding protein and design of a protein with higher affinity, *J. Am. Chem. Soc.*, 2014, **136**(50), 17484–17494.
122 Y. Yuan, Q. Yu, J. Wen, C. Li, Z. Guo, X. Wang and N. Wang, Ultrafast and Highly Selective Uranium Extraction from Seawater by Hydrogel-like Spidroin-based Protein Fiber, *Angew. Chem., Int. Ed.*, 2019, **58**(34), 11785–11790.
123 NEA & IAEA, *Uranium: Resources, Production and Demand 2024*, OECD Publishing, Paris, 2025.
124 C. Tsouris, Uranium extraction: Fuel from sewater, *Nat. Energy*, 2017, **2**, 17022.
125 Q. Sun, B. Aguila, J. Perman, A. S. Ivanov, V. S. Bryantsev, L. D. Earl, C. W. Abney, L. Wojtas and S. Ma, Bio-inspired nano-traps for uranium extraction from seawater and recovery from nuclear waste, *Nat. Commun.*, 2018, **9**, 1644.
126 T. Mizumachi, M. Sato, M. Kaneko, T. Takeyama, S. Tsushima and K. Takao, Fully Chelating N_3O_2-Pentadentate Planar Ligands Designed for the Strongest and Selective Capture of Uranium from Seawater, *Inorg. Chem.*, 2022, **61**, 6175–6181.
127 K. Takao, How does chemistry contribute to circular economy in nuclear energy systems to make them more sustainable and ecological?, *Dalton Trans.*, 2023, **52**, 9866–9881.
128 H. Moll, F. Lehmann and J. Raff, Interaction of curium(III) with surface-layer proteins from Lysinibacillus sphaericus JG-A12, *Colloids Surf., B*, 2020, **190**, 110950.
129 H. D. Lee, C. J. Grady, K. Krell, C. Strebeck, A. Al-Hilfi, B. Ricker, M. Linn, N. Y. Xin, N. M. Good, N. C. Martinez-Gomez and A. A. Gilad, A novel protein for bioremediation of gadolinium waste, *Protein Sci.*, 2025, **34**(4), e70101.
130 T. Cheisson and E. J. Schelter, Rare earth elements: Mendeleev's bane, modern marvels, *Science*, 2019, **363**, 489–493.
131 Z. Dong, J. A. Mattocks, J. A. Seidel, J. A. Cotruvo Jr. and D. M. Park, Protein-based approach for high-purity Sc, Y, and grouped lanthanide separation, *Sep. Purif. Technol.*, 2023, **333**, 125919.
132 G. Creff, C. Zurita, A. Jeanson, G. Carle, C. Vidaud and C. Den Auwer, What do we know about actinides-proteins interactions?, *Radiochim. Acta*, 2019, **107**(9–11), 993–1009.
133 M. Ali, A. Kumar, M. Kumar and B. N. Pandey, The interaction of human serum albumin with selected lanthanide and actinide ions: Binding affinities, protein unfolding and conformational changes, *Biochemistry*, 2016, **123**, 117–129.
134 A. Jeanson, M. Ferrand, H. Funke, C. Hennig, P. Moisy, P. L. Solari, C. Vidaud and C. Den Auwer, The Role of Transferrin in Actinide(IV) Uptake: Comparison with Iron (III), *Chem. – Eur. J.*, 2010, **16**, 1378–1387.
135 M. Sturzbecher-Hoehne, C. Goujon, G. J. Deblonde, A. B. Mason and R. J. Abergel, Sensitizing curium luminescence through an antenna protein to investigate biological actinide transport mechanisms, *J. Am. Chem. Soc.*, 2013, **135**(7), 2676–2683.
136 C. Zurita, S. Tsushima, P. L. Solari, D. Menut, S. Dourdain, A. Jeanson, G. Creff and C. Den Auwer, Interaction Between the Transferrin Protein and Plutonium (and Thorium), What's New?, *Chem. – Eur. J.*, 2023, **29**(55), e202300636.
137 C. Zurita, S. Tsushima, C. Bresson, M. G. Cortes, P. L. Solari, A. Jeanson, G. Creff and C. Den Auwer, How Does Iron Storage Protein Ferritin Interact with Plutonium (and Thorium)?, *Chem. – Eur. J.*, 2021, **27**(7), 2393–2401.
138 C. Zurita, S. Tsushima, P. L. Solari, A. Jeanson, G. Creff and C. Den Auwer, Interaction of Th(IV), Pu(IV) and Fe(III)

with ferritin protein: how similar?, *J. Synchrotron Radiat.*, 2022, **29**, 45–52.

139 A. Kumar, M. Ali, R. S. Ningthoujam, P. Gaikwad, M. Kumar, B. B. Nath and B. N. Pandey, The interaction of actinide and lanthanide ions with hemoglobin and its relevance to human and environmental toxicology, *J. Hazard. Mater.*, 2016, **307**, 281–293.

140 G. Zhu, M. Tan, Y. Li, X. Xiang, H. Hu and S. Zhao, Accumulation and Distribution of Uranium in Rats after Implantation with Depleted Uranium Fragments, *J. Radiat. Res.*, 2009, **50**, 183–192.

141 G. Creff, S. Safi, J. Roques, H. Michel, A. Jeanson, P.-L. Solari, C. Basset, E. Simoni, C. Vidaud and C. Den Auwer, Actinide (IV) Deposits on Bone: Potential Role of the Osteopontin-Thorium Complex, *Inorg. Chem.*, 2016, **55**(1), 29–36.

142 B. Li, J. Raff, A. Barkleit, G. Bernhard and H. Foerstendorf, Complexation of U(VI) with highly phosphorylated protein, phosvitin: A vibrational spectroscopic approach, *J. Inorg. Biochem.*, 2010, **104**(7), 718–725.

143 S. Kumar, G. Creff, C. Hennig, A. Rossberg, R. Steudtner, J. Raff, C. Vidaud, F. R. Oberhaensli, M. D. Bottein and C. Den Auwer, How Do Actinyls Interact with Hyperphosphorylated Yolk Protein Phosvitin?, *Chem. – Eur. J.*, 2019, **25**(53), 12332–12341.

144 H. Zänker, K. Heine, S. Weiss, V. Brendler, R. Husar, G. Barnhard, K. Gloe, T. Henle and A. Barkleit, Strong Uranium(VI) Binding onto Bovine Milk Proteins, Selected Protein Sequences, and Model Peptides, *Inorg. Chem.*, 2019, **58**(7), 4173–4189.

145 G. J.-P. Deblonde, J. A. Mattocks, H. Wang, E. M. Gale, A. B. Kersting, M. Zavarin and J. A. Cotruvo Jr., Characterization of Americium and Curium Complexes with the Protein Lanmodulin: A Potential Macromolecular Mechanism for Actinide Mobility in the Environment, *J. Am. Chem. Soc.*, 2021, **143**(38), 15769–15783.

146 É. Ansoborlo, B. Amekraz, C. Moulin, V. Moulin, F. Taran, T. Bailly, R. Burgada, M.-H. Hengé-Napoli, A. Jeanson, C. Den Auwer, L. Bonin and P. Moisy, Review of actinide decorporation with chelating agents, *C. R. Chim.*, 2007, **10**, 1010–1019.

147 Y. Li, B. Li, L. Chen, J. Dong, Z. Xia and Y. Tian, Chelating decorpporation agents for internal contamination by actinides: Designs, mechanisms, and advances, *J. Inorg. Biochem.*, 2023, **238**, 112304.

148 A. Heller, C. Senwitz, H. Foerstendorf, S. Tsushima, L. Holtmann, B. Drobot and J. Kretzschmar, Europium(III) Meets Etidronic Acid (HEDP): A Coordination Study Combining Spectroscopic, Spectrometric, and Quantum Chemical Methods, *Molecules*, 2023, **28**, 4469.

149 N. A. Fitriyanto, M. Fushimi, M. Matsunaga, A. Pertiwiningrum, T. Iwama and K. Kawai, Molecular structure and gene analysis of Ce^{3+}-induced methanol dehydrogenase of Bradyhizobium sp. MAFF211645, *J. Biosci. Bioeng.*, 2011, **111**(6), 613–617.

150 T. Nakagawa, R. Mitsui, A. Tani, K. Sasa, S. Tashiro, T. Iwama, T. Hayakawa and K. Kawai, A Catalytic Role of XofX1 as La^{3+}-Dependent Methanol Dehydrogenase in Methylbacterium extoquens Strain AM1, *PLoS One*, 2012, 7(11), e50480.

151 A. Pol, T. R. M. Barends, A. Dietl, A. F. Khadem, J. Eygensteyn, M. S. M. Jetten and H. J. M. Op den Camp, Rare earth metals are essential for methanotrophic life in volcanic mudpots, *Environ. Microbiol.*, 2014, **16**(1), 255–264.

152 H. Lumpe, A. Pol, H. J. M. Op den Camp and L. J. Daumann, Impact of the lanthanide contraction on the activity of a lanthanide-dependent methanol dehydrogenase – a kinetic and DFT study, *Dalton Trans.*, 2018, **47**, 10463–10469.

153 M. Y. Voutsinos, J. F. Banfield and H.-L. O. McClelland, Extensive and diverse lanthanide-dependent metabolism in the ocean, *ISME J.*, 2025, **19**(1), wraf057.

154 R. Bros, J. Carpena, V. Sere and A. Beltritti, Occurrence of Pu and Fissiogenic REE in Hydrothermal Apatites from the Fossil Nuclear Reactor at Oklo (Gabon), *Radiochim. Acta*, 1996, **74**, 277–282.

155 G. J.-P. Deblonde, J. A. Mattocks, Z. Dong, P. T. Wooddy, J. A. Cotruvo Jr. and M. Zavarin, Capturing an elusive but critical element: Natural protein enables actinium chemistry, *Sci. Adv.*, 2021, 7(43), eabk0273.

156 G. J.-P. Deblonde, K. Morrison, J. A. Mattocks, J. A. Cotruvo Jr., M. Zavarin and A. B. Kersting, Impact of a Biological Chelator, Lanmodulin, on Minor Actinide Aqueous Speciation and Transport in the Environment, *Environ. Sci. Technol.*, 2023, **57**(49), 20830–20843.

157 H. Singer, B. Drobot, C. Zeymer, R. Steudtner and L. J. Daumann, Americium preferred: lanmodulin, a natural lanthanide-binding protein favors an actinide over lanthanides, *Chem. Sci.*, 2021, **12**, 15581–15587.

158 J. A. Mattocks, J. A. Cotruvo Jr. and G. J.-P. Deblonde, Engineering lanmodulin's selectivity for actinides over lanthanides by controlling solvent coordination and second-sphere interactions, *Chem. Sci.*, 2022, **13**, 6054–6066.

159 J. A. Mattocks, J. J. Jung, C.-Y. Lin, Z. Dong, N. H. Yennwar, E. R. Featherston, C. S. Kang-Yun, T. A. Hamilton, D. M. Park, A. K. Boal and J. A. Cotruvo, Enhanced rare-earth separation with a metal-sensitive lanmodulin dimer, *Nature*, 2023, **618**, 87–93.

160 J. L. Hemmann, P. Keller, L. Hemmerle, T. Vonderach, A. M. Ochsner, M. Bortfeld-Miller, D. Günther and J. A. Vorholt, *J. Biol. Chem.*, 2023, **299**(3), 102940.

161 M. Wehrmann, P. Billard, A. Martin-Meriadec, A. Zegeye and J. Klebensberger, Functional Role of Lanthanides in Enzymatic Activity and Transcriptional Regulation of Pyrroloquinoline Quinone-Dependent Alcohol Dehydrogenases in Pseudomonas putida KT2440, *mBio*, 2017, **8**(3), e00570–e00517.